ZIRAT-11 Annual Report

Authors

Ron Adamson,
Zircology Plus, Fremont, Pleasanton, CA, USA

Brian Cox,
University of Toronto, Ontario, Canada

Friedrich Garzarolli,
Erlangen, Germany

Rolf Riess,
NPC Neunkirchen, Germany

George Sabol,
Export, Pennsylvania, USA

Alfred Strasser,
Aquarius Services Corp., Sleepy Hollow, NY, USA

Peter Rudling,
Advanced Nuclear Technology International Europe AB,
Skultuna, Sweden

November 2006

Advanced Nuclear Technology International
Krongjutarvägen 2C, SE-730 50 SKULTUNA
Sweden

info@antinternational.com
www.antinternational.com

DISCLAIMER

The information presented in this report has been compiled and analysed by Advanced Nuclear Technology International Europe AB (*ANT* International) and its subcontractors. *ANT* International has exercised due diligence in this work, but does not warrant the accuracy or completeness of the information. *ANT* International does not assume any responsibility for any consequences as a result of the use of the information for any party, except a warranty for reasonable technical skill, which is limited to the amount paid for this assignment by each *ZIRAT* program member.

ACRONYMS AND EXPLANATIONS

AD●PT	Advanced Doped Pellet Technology
AECL	Atomic Energy of Canada Limited
ANL	Argonne National Laboratory
ANT	Advanced Nuclear Technology
A●A	Axial ●ffset Anomaly
APSR	Axial Power Shaping Rods
ASME	American Society of Mechanical Engineers
ASLB	Atomic Safety and Licensing Board
ASTM	American Society for Testing and Materials
B&W	Babcock&Willcox
BIA	Bureau of Indian Affairs
BLG	Brennelement-Lager Gorleben
BLM	Bureau of Land Management
B●C	Beginning of Cycle
B●R	Research Fast Reactor
BWR	Boiling Water Reactor
BZA	Brennelement-Zwischenlager Ahaus
CANDU	CANada Deuterium Uranium
CEA	Commissariat à l'Energie Atomique
CEZUS	Companie Europen Ziconium Ugine Sandvik
CGR	Crack Growth Rate
CILC	Crud Induced Localized Corrosion
CIPS	Crud Induced Power Shifts
CPR	Critial Power Ratio
CREA	Control Rod Ejection Accident
CRDA	Control Rod Drop Accident
CRUD	Chalk River Unidentified Deposits
CSED	Critical Strain Energy Density
CWSRA	Cold Work and Stress Relieved Annealed???
CZP	Cold Zero Power
DHC	Delayed Hydride Cracking
DNBR	Departure from Nucleate Boiling Ratio
D●	Dissolved ●xygen
DX	Duplex
EBS	Engineered Barrier System
ECP	Electrochemical Corrosion Potential
EFFPD	EFfective Full Power Days
ELS	Extra-Low Sn
ENS	European Nuclear Society
E●C	End of Cycle
E●L	End ●f Life
ESSC	Enhanced Spacer Shadow Corrosion
FA	Fuel Assembly
FCC	Face Centered Cubic
FDS	Fire Dynamics Simulator
FEM	Finite Element Analysis
FGR	Fission Gas Release
FRED	Fuel Reliability Data Base
GE	General Electric
GNF	Global Nuclear Fuel
GT	Guide Tube
GTAW	Gas Tungsten Arc
GTS	Grimsel Test Site
HAZ	Heat Affected Zone

HBS	High Burnup Structure
HCP	Hexagonal Close-Packed
HDCI	High Duty Core Index
HF	High Frequency
HLW	High Level Waste
HPA	High Performance Alloy
HPUF	Hydrogen PickUp Fraction
HTP	High Thermal Performance
HWC	Hydrogen Water Chemistry
HZP	Hot Zero Power
IAEA	International Atomic Energy Agency
IFA	Instrumented Fuel Assemblies
IGSCC	Intergranular Stress Corrosion Cracking
ISFSI	Independent Spent Fuel Storage Installations
ISG	Interim Staff Guidance documents
IZNA	Information on Zirconium Alloys
KKG	KernKraftwerk Gösgen
KKL	KernKraftwek Leibstadt
KWU	KraftWerkUnion
LHGR	Linear Heat Generation Rate
LK	Låg corrosion (Low Corrosion in Swedish)
LOCA	Loss of Coolant Accident
LTA	Lead Test Assemblies
LTP	Low-Temperature Process
LWR	Light Water Reactor
MDA	Mitsubishi Developed Alloy
MELLLA	Maximum Extended Load Line Analysis
MHI	Mitsubishi Heavy Industries
MOX	Mixed Oxide
MPC	Multi-Purpose Canister
NDA	New Developed Alloy
NFI	Nuclear Fuel Industries
NIST	National Institute of Standards
NMC	Noble Metal Chemistry
NMCA	Noble Metal Chemical Addition
NPP	Nuclear Power Plant
NRC	Nuclear Regulatory Commission
NSRR	Nuclear Safety Research Reactor
NWC	Normal Water Chemistry
OPG	Ontario Power Generation company
ORNL	Oak Ridge National Lab.
PCI	Pellet Cladding Interaction
PCMI	Pellet Cladding Mechanical Interaction
PFS	Private Fuel Storage
PGP	Particle Growth Parameter
PIE	Post-Irradiation Examinations
PWR	Pressurised Water Reactor
PWSCC	Primary Water Stress Corrosion Cracking
R&D	Research & Development
RBMK	Russian type Boiling Water Reactor
RCCA	Rod Cluster Control Assemblies
RCS	Reactor Coolant System
RCT	Ring Compression Rest
RHT	Radial Hydride Treatment
RIA	Reactivity Initiated Accident
ROW	Right of Ways

RPV	Reactor Pressure Vessel
RSK	Reaktor Sicherheits Kommission
RT	Room Temperature
RX	Recrystallised
RXA	Recrystallised Annealed
SCC	Stress Corrosion Cracking
SED	Strain-Energy Density
SEM	Scanning Electron Microscopy
SFPO	Spent Fuel Projects Office
SG	Steam Generator
SOCAP	Second Order Cumulative Annealing Parameter
SPP	Second Phase Particle
SRA	Stress Relieved Annealed
SRP	Standard Review Plan
SS	Stainless Steel
STR	Special Topic Report
TE	Total Elongation
TEM	Transmission Electron Microscopy
TFGR	Transient Fission Gas Release
TR	Technical Requirements
TSDE	Thermal Simulation of Drift Emplacement
TSS	Terminal Solid Solubility
URL	Underground Research Laboratories
UTS	Ultimate Tensile Strength
VVER	Voda Voda Energo Reactor (Russian type *PWR*)
ZIRAT	ZIRconium Alloy Technology
ZIRLO	ZIRconium Low Oxidation

UNIT CONVERSION

TEMPERATURE °C + 273,15 = K °C*1,8 +32 = °F		
T(K)	**T (°C)**	**T(°F)**
273	**0**	32
289	16	61
298	25	**77**
373	**100**	212
473	**200**	392
573	**300**	572
633	360	680
673	**400**	**752**
773	**500**	932
783	510	950
793	520	968
823	550	1022
833	560	1040
873	**600**	1112
878	605	1121
893	620	1148
923	650	1202
973	**700**	1292
1023	**750**	1382
1053	**780**	1436
1073	**800**	1472
1136	863	1585
1143	870	1598
1173	**900**	1652
1273	**1000**	1832
1343	1070	1958
1478	1204	**2200**

MASS	
kg	**lbs**
0,454	**1**
1	2,20

DISTANCE	
x (µm)	**x (mils)**
0,6	0,02
1	0,04
5	0,20
10	0,39
20	0,79
25	0,98
25,4	**1,00**
100	3,94

PRESSURE		
bar	**MPa**	**psi**
1	0,1	14
10	**1**	142
70	**7**	995
70,4	**7,04**	**1000**
100	10	1421
130	13	**1847**
155	15,5	2203
704	**70,4**	**10000**
1000	100	14211

STRESS INTENSITY FACTOR	
MPa√m	**ksi√inch**
0,91	**1**
1	1,10

CONTENTS

1 INTRODUCTION

The objective of the Annual Review of Zirconium Alloy Technology (*ZIRAT*) is to review and evaluate the latest developments in zirconium alloy technology as they apply to nuclear fuel design and performance.

The objective is met through a review and evaluation of the most recent data on zirconium alloys and to identify the most important new information and discuss its significance in relation to fuel performance now and in the future. Included in the review are topics on materials research and development, fabrication, component design, and in-reactor performance.

Within the *ZIRAT*-11 Program, the following technical meetings were covered:

- *IAEA* Technical Meeting on" Behaviour of high corrosion resistance Zr-based alloys", Argentina, October 24 -28, 2005
- *NRC* Regulatory Information Conference (RIC), Fuel Session, Washington DC, USA, Feb. 7, 2006
- KTG Conference, Dresden, Germany, March 2-3, 2006
- 18th Annual Regulatory Information Conference, Washington DC, USA, March 7-9, 2006
- Annual Meeting on Nuclear Technology 2006, Aachen, Germany May 16-18, 2006
- 2006 Nuclear Fuels and Structural Materials for the next Generation Nuclear Reactors (ICAPP'06), Embedded Topical sponsored by ANS, June 4-8, Reno, Nevada
- Contribution of Materials Investigations to Improve the Safety and Performance of *LWR*s, Fontevraud 6, France, September 18-22, 2006
- 15th Pacific Basin Nuclear Conference, Sydney, Australia, October 15-20, 2006
- International Conference on Water Chemistry of Nuclear Reactor Systems, Jeju Island, Korea, October 23-26, 2006
- Top Fuel Conference, Salamanca, Spain, October 22 to 26, 2006

The extensive, continuous flow of journal publications is being monitored by several literature searches of world-wide publications and the important papers are summarised and critically evaluated. This includes the following journals:

- Journal of Nuclear Materials,
- Nuclear Engineering and Design,
- Kerntechnik
- Metallurgical and Materials Transactions A
- Journal of Alloys and Compounds
- Canadian Metallurgical Quarterly

- Journal de Physique IV
- Journal of Nuclear Science and Technology
- Nuclear Science & Engineering
- Nuclear Technology

The primary issues addressed in the review and this report are zirconium alloy research and development, fabrication, component design, ex- and in-reactor performance including:

- Regulatory bodies and utility perspectives related to fuel performance issues, fuel vendor developments of new fuel design to meet the fuel performance issues.
- Fabrication and quality control of zirconium manufacturing, zirconium alloy systems.
- Mechanical properties and their test methods (that are not covered in any other section in the report).
- Dimensional stability (growth and creep).
- Primary coolant chemistry and its effect on zirconium alloy component performance.
- Corrosion and hydriding mechanisms and performance of commercial alloys.
- Cladding primary failures.
- Post-failure degradation of failed fuel.
- Cladding performance in postulated accidents (*LOCA*, *RIA*).
- Dry storage.
- Potential burnup limitations.
- Current uncertainties and issues needing solution are identified throughout the report.

Background data from prior periods have been included wherever needed. Most data are from non-proprietary sources; however, their compilation, evaluations, and conclusions in the report are proprietary to *ANT* International and *ZIRAT* members as noted on the title page.

The information within the *ZIRAT*-11 Program is either retrieved from the open literature or from proprietary information that *ANT* International has received the OK from the respective organisation to provide this information within the *ZIRAT*-program.

The authors of the report are Dr. Ron Adamson, Brian Cox, Professor Emiritus, University of Toronto; Mr. Al Strasser, President of Aquarius and, Mr. Peter Rudling, President of *ANT* International, Mr. Friedrich Garzarolli, Dr. Rolf Riess and Mr. George Sabol.

The work reported herein will be presented in three Seminars: one in Naples, Florida, on January 29- January 31, 2007 one in Valencia, Spain on February 12-14, 2007 and one in Japan in 2007.

The Term of *ZIRAT*-11 started on February 1, 2006 and ends on January 31, 2007.

2 BURNUP ACHIEVEMENTS AND FUEL PERFORMANCE ISSUES (ALFRED STRASSER)

2.1 TRENDS IN FUEL OPERATING CONDITIONS

2.1.1 General Trends

The technical advances in materials technology and computational modeling methods, spurred on by economic incentives, have continued to increase the demands on fuel performance levels and to put pressure on the regulatory bodies to license operations to ever higher burnups. The types of changes in *LWR* operating methods to achieve improved safety and economics have not changed in the past year and still include:

- Annual fuel cycles extended to 18 and 24 months,
- Discharge burnups increased from mid-30 to mid-50 GWD/MT batch average exposures by higher enrichments, increased number of burnable absorbers in the assemblies and in *PWR*s higher Li and B levels in the coolant
- Plant power uprates that ranged from 5 to 20%,
- More aggressive fuel management methods with increased enrichments and peaking factors,
- Reduced activity transport by Zn injection into the coolant,
- Improved water chemistry controls,
- Component life extension with hydrogen water chemistry (*HWC*) and noble metal chemistry (*NMC*) in *BWR*s.

2.1.2 Fuel Cycle Lengths

The trend for increased fuel cycle lengths has come to a near "equilibrium" in the US with *PWR*s operating at an average of 500 effective full power days (*EFFPD*) per cycle and *BWR*s an average of over 600 *EFFPD* per cycle. Nearly all the US *BWR*s are trending toward 24 month cycles. The older, lower power density *PWR*s have implemented the 24 month cycles, but fuel management limitations, specifically reload batch sizes required, have limited implementation of 24 month cycles in the high power density plants. The economics of 24 month cycles tend to become plant specific since they depend on the balance of a variety of plant specific parameters. The potential economic gains for cycle extension have decreased since the US has significantly reduced the downtimes for reloading and maintenance procedures.

Other countries that historically have had only one power demand peak in the winter compared to the two summer and winter power peaks in the US are also trending toward longer cycles as a result of changes in economics, maintenance practices and licensing procedures. As an example, among the French reactors there are now six 900 MW plants and twenty 1300 MW plants on 18 month cycles. The remaining plants, twenty eight 900 MW and four 1500 MW plants, are on annual cycles (Provost, 2006).

2.1.3 Burnup Extension

Improved economics of the fuel cycle are the incentives for extended burnups, and include the decreased amount of spent fuel assemblies to be handled. The economics of decreased assemblies could be impacted by the much longer cooling times required in spent fuel pools prior to on-site dry storage or transport to a storage facility as noted later. The average batch burnups in *PWR*s are approaching 50 GWD/MT and in *BWR*s in the mid-40 GWD/MT. The peak *PWR* assemblies are in the range of 60-72 GWD/MT and the *BWR* in the range of 52-62 GWD/MT. The burnups are currently limited by the regulatory agencies more than by technical limitations, except for lead test assemblies and rods. Some of the current regulatory limits are in GWD/MT:

USA	62.5	peak rod	Netherlands	60 peak rod
Finland	45	batch average	Sweden	60 assembly, 64 rod
France	52	peak assembly	Switzerland	75 peak pellet
Germany	65	peak assembly	Taiwan	60 peak rod (*PWR*)
Japan	55	peak assembly		54 peak assembly (*BWR*)

Economic analyses reported in past *ZIRAT* reports indicated that economic incentives for extending burnups beyond the 60-70 GWD/MT batch average range will disappear and that other incentives will be needed to go beyond this level. More recent analyses and statements confirm this and are worth summarizing. In reviewing these estimates and modeling methods, the variability in results based on the in-put values and the methodology used should be recognized.

The biggest block to increasing burnup is the essentially universal regulatory limit on 5.00% initial uranium enrichment. Analyses for a variety of reactors that include *PWR*s (Westinghouse and *VVER*) and a *BWR* (*GE*) show that a 5% enrichment will provide up to 55 GWD/MT (*VVER*) and about 63 GWD/MT (*BWR*) *assembly* average burnup (Figure 2-1) (NEA, 2006). Advanced, sophisticated fuel management methods can probably raise this close to 70 GWD/MT, but are unlikely to exceed this level. A *GNF estimate for BWRs* states that 5% enrichment is equivalent to about 55 GWD/MT *batch* average burnup (Fawcett, 2006). The cost of equipping and licensing the industry to handle enrichments greater than 5% would be very great and time consuming; such a move is not being considered for the foreseeable future.

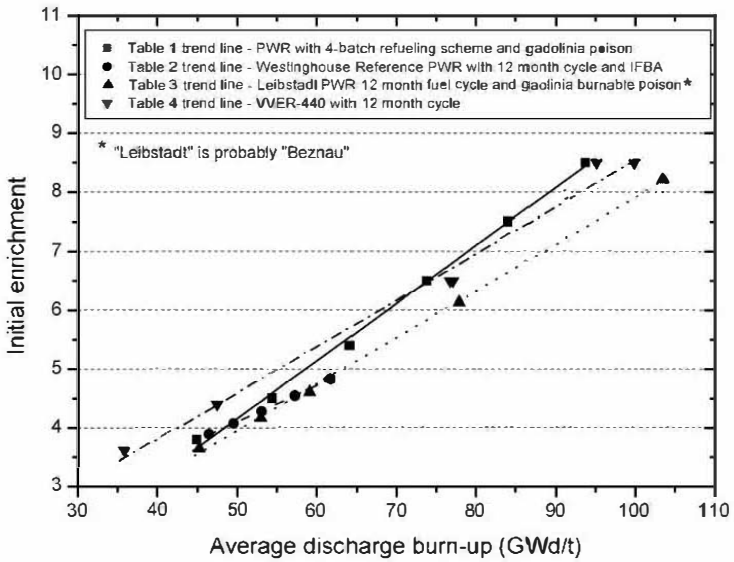

Figure 2-1: Initial Assembly Average Enrichment Required to Reach Goal Burnup (NEA, 2006).

2.1.4 Fuel Cycle Economics

Assuming the 5% enrichment limit can be overcome, is there an economic incentive to go to higher burnups? Recent economic analyses confirm previous analyses that the fuel cycle cost vs. burnup curve is either essentially flat or increases in cost with increasing burnup and is very sensitive to input parameters.

Fuel cycle cost analyses as a function of burnup were made for a *3 loop Westinghouse PWR* for 3, 4 and 5 batch fraction reloading schemes up to 100 GWD/MT assembly average discharge burnup at equilibrium(Gregg, 2005). Gadolinia was used as the burnable absorber in the cores. An $F_{\Delta H}$ of 1.585 was selected for all analyses and while this is quite high, it was assumed that improvements in materials and design would permit such higher peaking in the core. The increasing peaking factors with increasing burnup are shown on Figure 2-2. The cost components of the fuel cycle show the increase in the fuel costs with increasing enrichment and ore requirements and the decrease of the other costs due to the decreased number of assemblies fabricated (Figure 2-3).

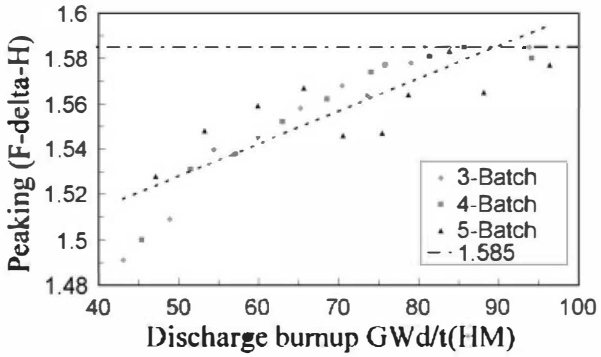

Figure 2-2: $F_{\Delta H}$ Versus Average Assembly Discharge Burnup for Three-, Four-, and Five- Batch Loading Patterns. (Gregg, 2005)

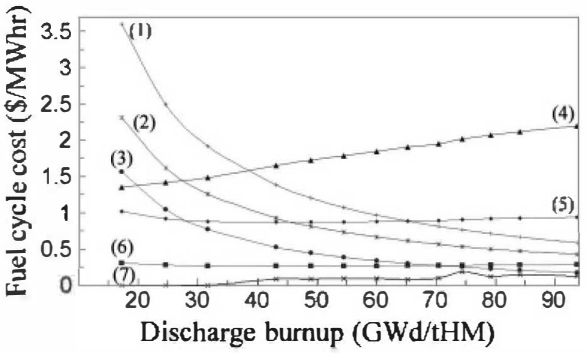

Figure 2-3: Typical Levelized Fuel Cost vs. Burnup Assuming Constant Unit Cost with Enrichment: (1) conditioning and final disposal costs, (2) fabrication costs, (3) transportation costs, (4) enrichment costs, (5) ore costs, (6) conversion costs, and (7) gadolinia costs (Gregg, 2005)

The unit costs assumed are given in Table 2-1 and are held constant with burnup in an optimistic (and unrealistic) case and a burnup dependent increase case given in Table 2-2. Note that uranium ore costs have about doubled since this publication and other costs have gone up somewhat as well making this case even more optimistic in general.

Table 2-1: Economics Parameters Assumed in the *PWR* Fuel Cycle Cost Study (Gregg, 2005).

Ore cost ($/kg U)[a]	25	Ore purchasing lead time (yr)	2
Conversion cost ($/kg U)	8	Conversion lead time (yr)	1.5
Enrichment cost ($/SWU)	90	Enrichment lead time (yr)	1
Fabrication cost ($/kg U)	275	Fabrication lead time (yr)	0.5
Transport cost ($/kg HM)	370	Transportation lag time (yr)	5
Conditioning/final disposal ($/kg HM)	1245	Conditioning/final disposal lag time (yr)	40
Provisioning rate (%)[b]	2.5	Discount rate (%)	11

[a]Ore, conversion, and enrichment costs are based on current day values. Transport, conditioning/final disposal, fabrication costs, and lead times from a 1994 Organization for Economic Cooperation and Development report.[3]
[b]Provisioning rate used to calculate conditioning and final disposal costs. Discount rate used for other costs.

Table 2-2: Burnup-Dependent Economics Parameters: Percent Increase from 50 to 100 GWd/tonne HM (Gregg, 2005).

Conversion cost (%)	0	Transport cost (%)	30
Enrichment cost (%)	0	Conditioning/final disposal cost (%)	30
Fabrication cost (%)	30		

The results show that the fuel cycle costs reach a minimum between 60 and 70 GWD/MT assembly average for both optimistic and more realistic burnup dependent cost cases. The costs in the optimistic case stay level after the minimum (Figure 2-4(a)) and in the more realistic case increase slightly after the minimum (Figure 2-4(b)).

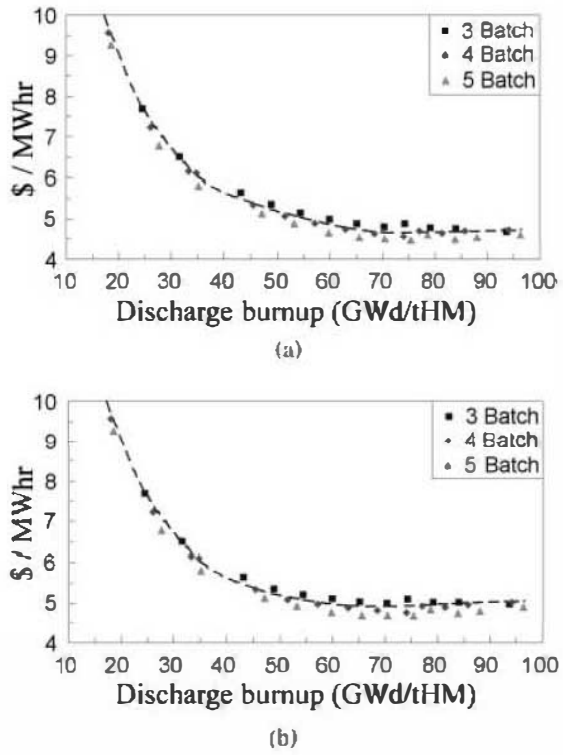

Figure 2-4: Levelized Fuel Cost vs. Discharge Burnup Assuming Units Costs (a) do not vary with enrichment/discharge burnup and (b) increase with enrichment/discharge burnup. (Gregg, 2005)

An even more detailed study of a 4 loop, 1200 MWe Westinghouse plant by the same organization, Nexia Solutions/BNFL, evaluated 4 cases with reloads containing gadolinia burnable absorbers (NEA, 2006):

- Burnup *independent* unit costs and (1) optimistic enrichment, (2) pessimistic enrichment,
- Burnup *dependent* unit costs and (1) optimistic enrichment, (2) pessimistic enrichment.

The optimistic and pessimistic enrichments for the fuel cycles are shown on Table 2-3; the optimistic cycles are with no gadolinia residual penalty and the pessimistic ones include the penalty. The burnup independent costs were modified from the previous case by increasing the ore costs from $25 to a more currently reasonable $50/KgU and the fabrication costs from $275 to $300/kg/U. The burnup dependent costs are given in Table 2-4. The other major variable applied was the monetary discount rate at 0%, 5% and 10% to show the effect of currency fluctuations and accounting practices.

Table 2-3: Optimistic and Pessimistic Enrichment Assumptions (NEA, 2006)

Fuel cycle parameters for optimistic scenario

Burn-up	Initial enrichment (w/o)	Cycle length (months)	Refuelling fraction
45	3.841	12.0	0.268
55	4.481	12.0	0.218
65	5.102	12.0	0.186
75	5.785	12.0	0.161
85	6.495	12.0	0.142
95	7.258	12.0	0.127

Fuel cycle parameters for pessimistic scenario

Burn-up	Initial enrichment (w/o)	Cycle length (months)	Refuelling fraction
45	3.8	11.4	0.25
55	4.5	13.9	0.25
65	5.4	16.4	0.25
75	6.5	19.0	0.25
85	7.5	21.5	0.25
95	8.5	24.0	0.25

Table 2-4: Burnup Dependent Cost Inputs

Burn-up dependent fabrication cost (linear escalation)

Burn-up	$/kgU
45	300
55	330
65	360
75	390
85	420
95	450

Burn-up dependent spent fuel transport cost (escalation proportional to burn-up)

Burn-up	$/kgU
45	230
55	280
65	330
75	380
85	430
95	480

Burn-up dependent encapsulation/disposal cost (escalation proportionalto burn-up)

Burn-up	$/kgU
45	610
55	745
65	880
75	1 015
85	1 150
95	1 290

The most optimistic case with optimistic enrichment and burnup independent unit costs was the only one that had fuel cycle costs level off with burnup after reaching a minimum between 60 and 70 GWD/MT (Figure 2-5). All other cases increased in cost with burnup after reaching this or an earlier minimum. The pessimistic enrichment/burnup *independent* cost curves are shown on Figure 2-6and the pessimistic enrichment/burnup *dependent* curve on Figure 2-7.

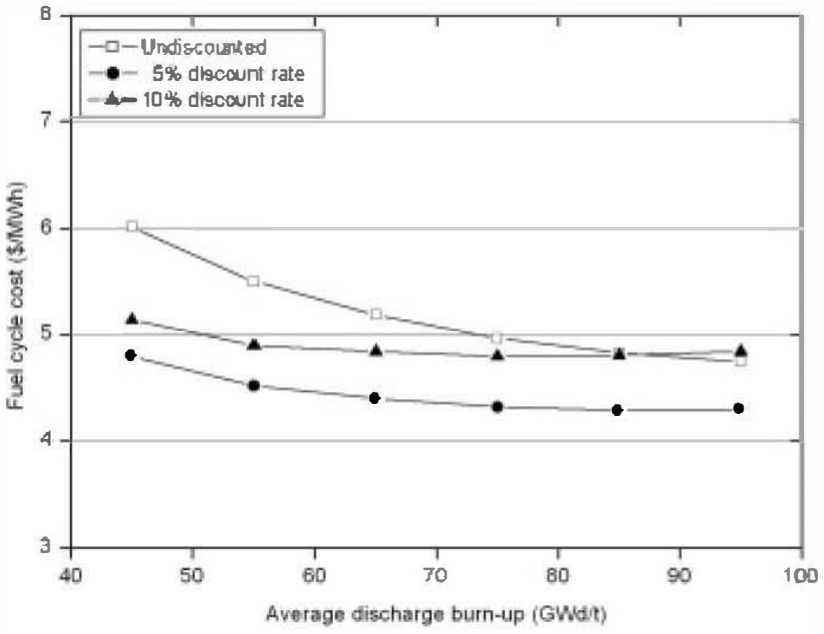

Figure 2-5: Fuel Cycle Levelised Cost vs. Average Discharge Burn-up and Discount Rate – Optimistic Initial Enrichment/Burn-up Relation and Burn-up-independent Unit Costs. (NEA, 2006)

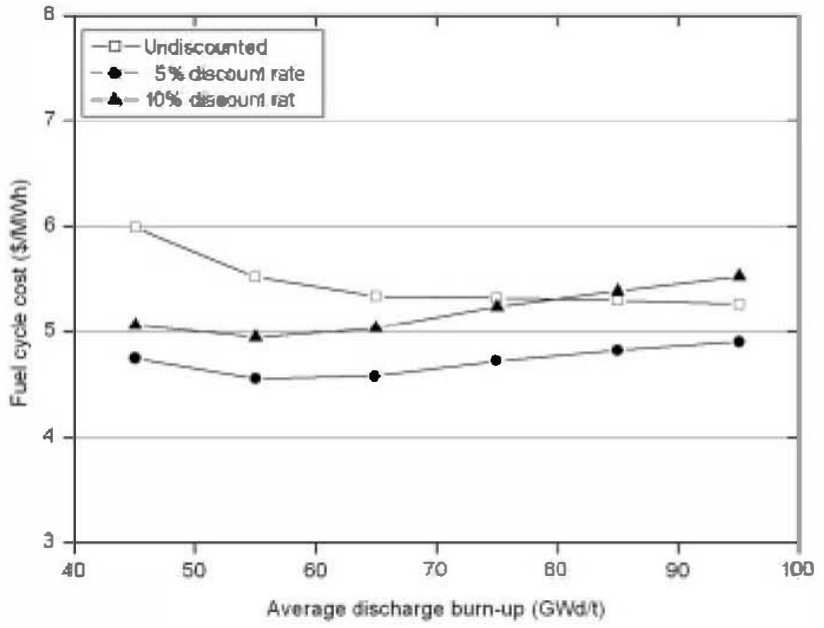

Figure 2-6: Fuel Cycle Levelised Cost vs. Average Discharge Burn-up and Discount Rate – Pessimistic Initial Enrichment/Burn-up Relation and Burn-up-independent Unit Costs (NEA, 2006)

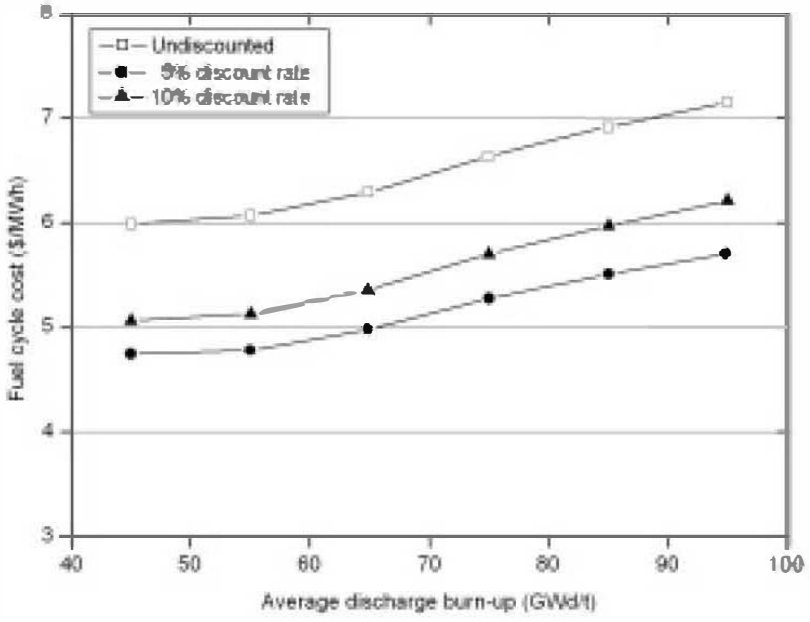

Figure 2-7: Fuel Cycle Levelized Cost vs. Average Discharge Bum-up and Discount Rate – Pessimistic Initial Enrichment/Bum-up Relation and Bum-up-dependent Unit Costs. (NEA, 2006)

The previous analyses were done with the FCE fuel cycle cost code. Analyses of the same cases with the DANESS fuel cycle cost code showed the same trends.

An analysis of the *WWER-440 PWR* economics vs. bumup was made by KFKI, Hungary and also available in the same report (NEA, 2006). The bases of the analyses were different than for the Westinghouse plants and included:

- Two types of fuel cycles: one with increased boron concentration and one with gadolinia absorbers,
- Fixed cycle length instead of fixed batch size,
- $700 fabrication penalty per gadolinia pin,
- 0% Discount in cost calculations as customary in Hungary,
- Optimistic and pessimistic analyses as per Table 2-5, different from Westinghouse.

Table 2-5: Input to *VVER*-440 Economic Analyses (NEA, 2006)

(a) VVER-440 cycle characteristics

No. of feed assemblies	Average assembly discharge burn-up (MWd/t)	Average initial ^{235}U enrichment (w/o)	No. of fuel rods per assembly containing gadolinia burnable poison
102	35.9	3.6	0
77	48.3	4.4	0
48	77.5	6.5	0
37	100.5	8.5	0
78	47.7	4.4	3
49	75.9	6.5	12
40	92.9	8.5	24

(b) VVER-440 sample economic scenarios

	Optimistic scenario	Pessimistic scenario
Uranium ore price ($/kg)	25	40
Enrichment cost ($/kgSWU)	80	95
Fabrication cost/assembly ($)	50 000	40 000
Back-end cost/assembly ($)	60 000	60 000

The results show a greater incentive for very high burnups in WWERs than Westinghouse plants (Figure 2-8) although the undiscounted cost calculations help in that respect. The fuel cycles with burnable absorbers have a minimum at about 75-80 GWD/MT and without absorbers the cost keeps decreasing up to the 100 GWD/MT; however, operating a core with 8.5% enrichment without burnable absorbers seems unrealistic.

The *BWRs are currently approaching the 5% enrichment limit* in order to achieve 24 month cycles and plant uprates as high as 20%. A typical assembly design containing a large number of fuel rods with 4.95% enrichment and 8.00% gadolinia rods for reactivity holddown is shown in Figure 2-9 (Brown, 2005). The necessary core reactivity to provide this energy leads to large batch sizes which in turn lead to lower batch average burnups; in this case from >50 GWD/MT to about 44 GWD/MT (Table 2-6). In order to operate these cores at full economical potential, the authors point out that the 5.00% enrichment limit will have to be exceeded by relatively small increases to 5.2% and 5.4% for some of the rods. The large number of 4.95% enriched rods instead of fewer number of >5% enriched rods decreases the ability to optimize the local power peaking in the bundle relative to the critical power ratio (*CPR*) and the linear heat generation rate (*LHGR*) and lead to a less efficient core design.

The economic and burnup gains are also shown in Table 2-7, based on cost parameters in Table 2-7 that no longer represent levels in 2006, but still support the trend in the right direction.

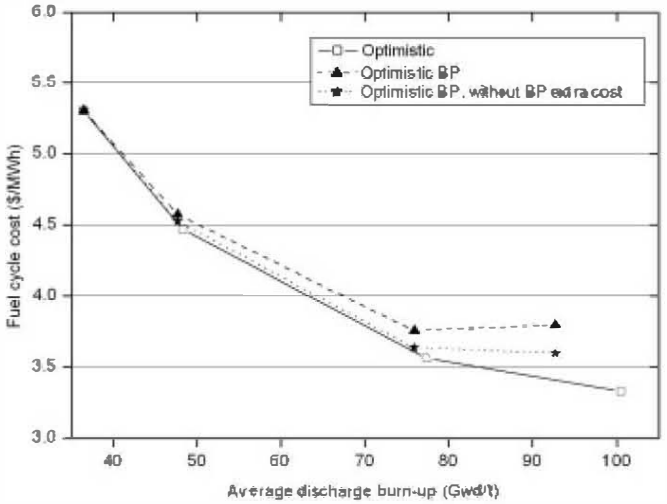

Figure 2-8: Comparison of the Total Fuel Cycle With and Without the Extra Gadolinia Cost (Optimistic Scenario) in *VVER*-44● (NEA, 2●●6)

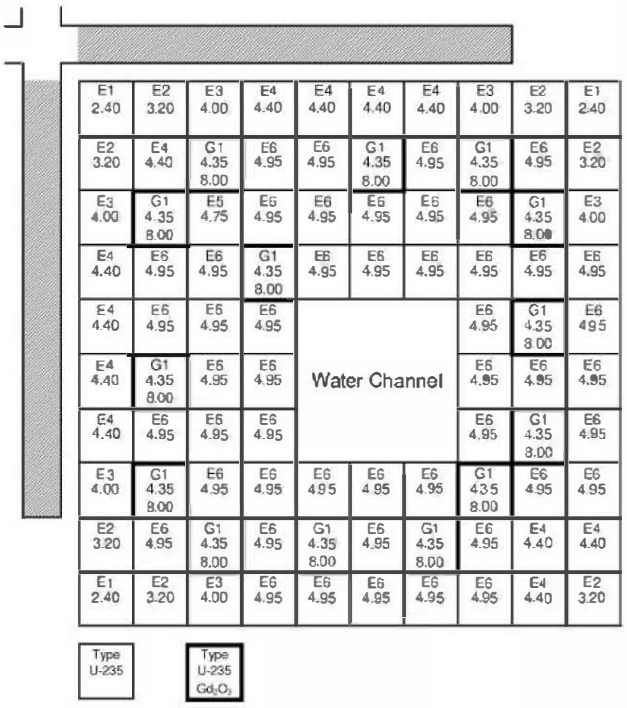

Pellet Type	Quantity	U-235 + Gd_2O_3 Concentration (wt% percent)
E1	3	2.40
E2	7	3.20
E3	6	4.00
G1	14	4.35 + 8.00
E4	12	4.40
E5	1	4.75
E6	48	4.95

Figure 2-9: Example Lattice Enrichment Map for 2-yr/12●% Uprate Cycle (Brown, 2●●5).

Table 2-6: Fuel Burnup and Fuel Cycle Cost Comparison *BWR*/4, 764 Fuel Assembly, D-Lattice, 24-Month Cycles (Brown, 2005)

Case	Average/ Maximum Enrichment, wt% ^{235}U	Percent Nameplate Power (Power Density, kW/ℓ)	Reload Batch Size, Fuel Assembly (Percent of Core)	Batch Average Discharge Exposure (GWd/tonne U)	Relative Fuel Cycle Cost	Approximate Savings per Reload Batch ($)
1 (No uprate)	4.40/4.95	105 (51.1)	260 (34%)	52	0.98	—
2 (Uprate, low burnup)	4.10/4.95	120 (58.7)	348 (46%)	44	1.00	Base
3 (Uprate, medium burnup) IDEAL A	4.31/5.2	120 (58.7)	320 (42%)	48	0.98	2.2 million
4 (Uprate, high burnup) IDEAL B	4.56/5.4	120 (58.7)	292 (38%)	52	0.97	2.9 million

*PPC for cases 1 and 2 are about the same. PPC [mills/kW·h(electric)] is defined as the sum of capital carrying costs, operating and maintenance costs, and fuel cycle costs.

Table 2-7: Fuel Cycle Cost Study Inputs for *BWR* (Brown, 2005).

Uranium and Financing Parameters	
U_3O_8 cost	\$12/lb U_3O_8
Conversion cost	\$4/kg U
Enrichment cost	\$86/kg separative work unit
Tails assay	0.3 wt% ^{235}U
In-core interest	7%
Fuel disposal	1 mill/kW·h(electric)

2.1.5 Zinc Injection

One of the successful innovations in operating methods has been zinc (Zn) injection into the coolant to reduce activity transport within the primary coolant systems of both *PWR*s and *BWR*s, without significantly affecting cladding corrosion, be it Zircaloy-4, *ZIRLO* or M5. The presence of Zn, however, promotes the deposit of a Zn containing spinel on the cladding probably in the form of $Ni_xZn_yFe_zO_4$, especially if sufficient Fe is present. While these crud deposits have not been observed to affect corrosion of the cladding, they are suspected of promoting boron deposits that can result in axial offset anomalies (*AOA*s) also called crud induced power shifts (*CIPS*s) in plants with subcooled nucleate boiling. Plants without nucleate boiling have not observed any *AOA*s with the exception of Ft. Calhoun. A key question has therefore been the effect of Zn injection on cores with nucleate boiling and the experience of such plants with recently applied Zn injection.

The High Duty Core Index (*HDCI*) of the plants in question compared to some of the lower duty plants that have applied Zn injection are:

Gösgen	295
Vandellos 1&2	190-230
Asco 1&2	190-200
Vogtle 1&2	175
Callaway	170
Ft. Calhoun	118
Biblis B	109
Diablo Canyon	100
Farley	100
TMI	89
Biblis A	65

Vogtle 1, the highest duty US plant applying Zn injection, reported an *AOA* shortly after Zn injection started in its Cycle 12 in 2004. The Zn injection was not resumed after the Cycle 12 shutdown since it was believed there is a relationship between the Zn injection and the formation of the *AOA*.

Cycle 13 of Vogtle 1was started without Zn injection, but Zn injection was resumed after about 8 months. Within 2 weeks of the start of Zn injection there was evidence of an *AOA* and the Zn injection was shut off. The fuel was ultrasonically cleaned after Cycle 12, but the process could only remove about 65% of the crud (Loftin, 2006).

Vogtle 2, Cycle 12 was started with Zn injection, increasing the levels from 5 to 10 to 15 ppb, and there has been no evidence of *AOA* in this unit as of November, 2006. The units have identical thermal ratings and materials of construction. As of that date there have not been any differences in design or operating parameters identified between the two units. Plans are to make oxide measurements and crud analyses.

Ft. Calhoun is the only lower duty plant that has reported *AOA*s without crud and with Zn injection.

Gösgen, the highest duty plant among all *LWR*s, has been injecting Zn since 2004 and has reported that the fuel cladding has not been adversely affected, but has not made any statements about *AOA* experience (Rich, 2006). Since the plant has very low crud deposits as a result of low corrosion product input from their Incoloy 800 steam generator and operates with low boron content coolant with enriched boron they are significantly less prone to *AOA*s.

Gösgen has never observed any *AOA*s before or after Zn injection. However, they operate with low, 28% enriched ^{10}B, which is at the 950 ppm level at the beginning of their annual cycle. In addition they have not observed any crud deposits on their fuel.

Vandellos 2 started Zn injection in June, 2006 after reducing its average coolant temperature of 307.6°C (585.7°F) by 1.1°C (2°F) and its *HDCI* from 235 to 195 to decrease severity of its duty. Asco 2 started Zn injection in August, 2006. As of October, 2006 they reported that no *AOA*s had occurred (Sanchez, 2006).

The difference in performance of the two units will be of interest since Vandellos has Inconel 600 steam generators and Asco's are made of Incoloy 800 and prone to lower corrosion product input and crud buildup on fuel rods. The crud levels in these plants are not identified in the publication and the boron content is only stated as <1550 ppm. Low boron levels would of course help prevent *AOA* formations.

2.1.6 High Lithium Operation

The highest Li operation to date was implemented in Comanche Peak 2, Cycle 8 and consisted of a maximum 6 ppm Li to achieve a constant pH 7.4 throughout the cycle. This was preceded by the operation of Cycle 7 at a constant pH of 7.3 with a maximum 5 ppm Li (Iyer et al., 2006(b)). The Li histories for the two cycles are shown in Figure 2-10. The *EFFPD* for operation at 3.5 ppm Li or above was 334 for Cycle 8 and considerably higher than the 66 for Cycle 7. The nucleate boiling duties were considerably higher in Cycle 8 as well and had steaming rates about 25-30% higher than in Cycle 7.

Visual examinations and oxide measurements were made of rods from assemblies that operated in both cycles to 29-48 GWD/MT and in the Cycle 8 only to 25-28 GWD/MT. Oxide measurement ranges for the assemblies were:

Cycle 7+8	13-68 μ
Cycle 8	9-24 μ

Heavy brown crud with localized black crud could have affected the peak oxide measurements by the possible inclusion of some of the crud in the oxide measurements. The oxide thickness was generally at or below the predicted levels except for some higher values measured at the 120-140 inch (305-356 cm) elevations. The highest and lowest values after 2 cycles of irradiation are shown on Figure 2-11. The measurements are plotted against the overall *ZIRLO* data base on Figure 2-12 and indicate that they are at the upper bound of the data base.

The authors recommend that high duty plants proceed with caution if they plan to implement Li operations at these levels and that they include a surveillance program with such operations.

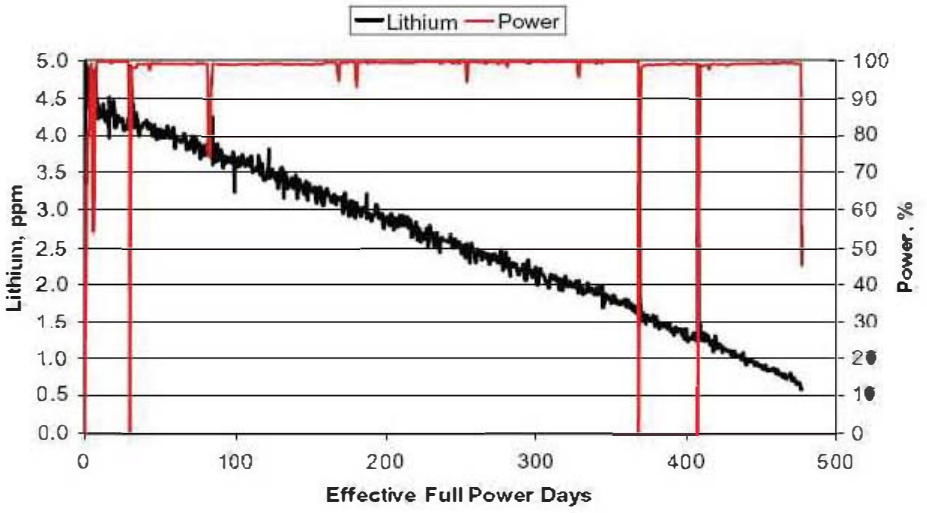

(a) Cycle 7 @ 5ppm Li max.

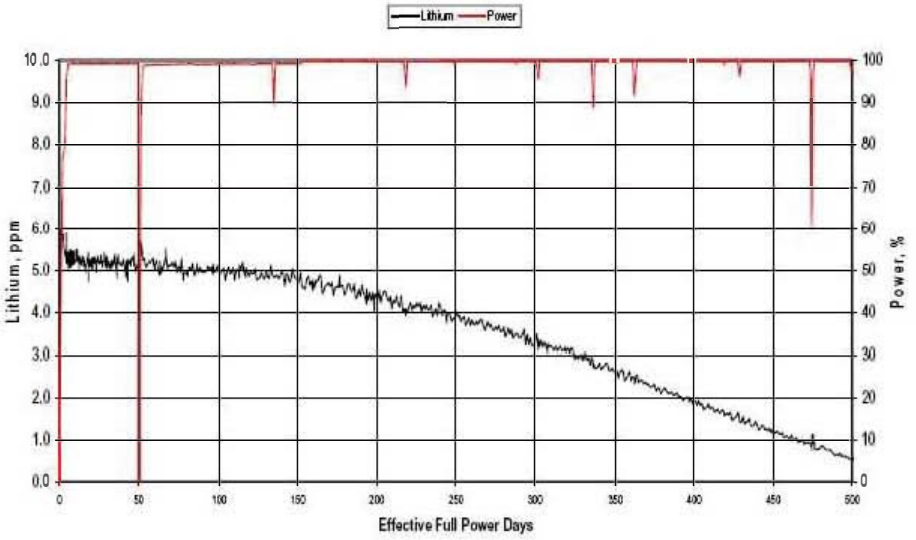

(b) Cycle 8 @ 6ppm Li max.

Figure 2-10: Lithium Levels in Comanche Peak Unit 2 (Iyer et al., 2006(b)).

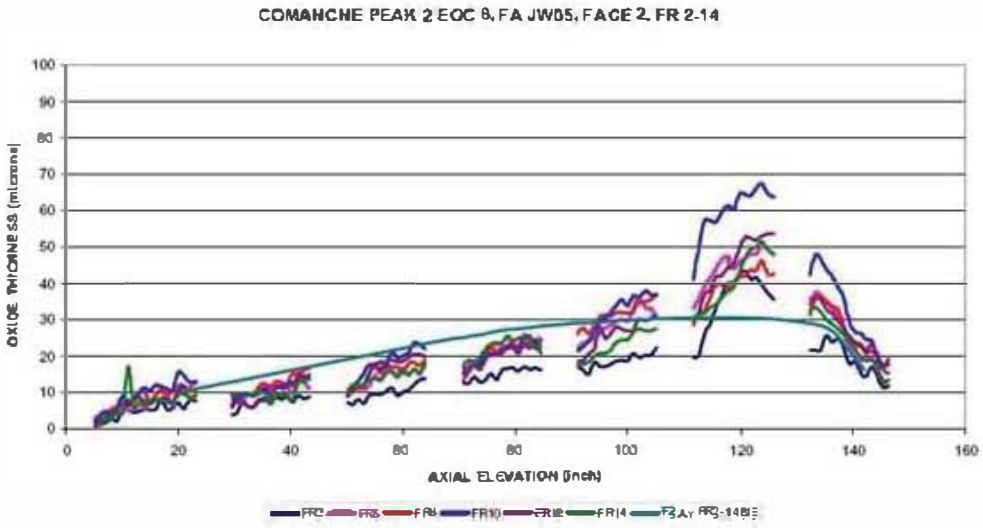

(a) Face 2, F/A JW05

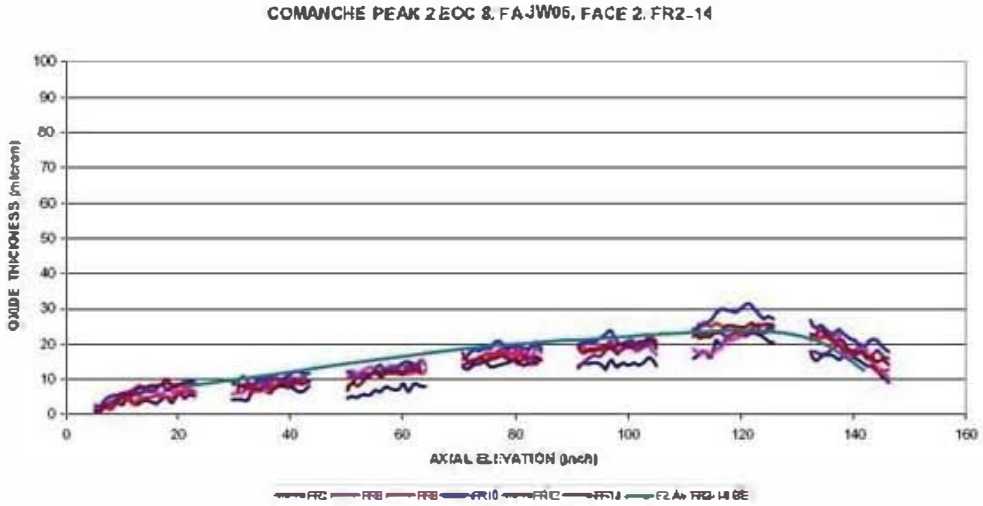

(b) Face 2 & 3, F/AJW06

Figure 2-11: Oxide Thickness as a Function of Elevation After Hight Lithium Operation for 2 Cycles. (Iyer et al., 2006(b))

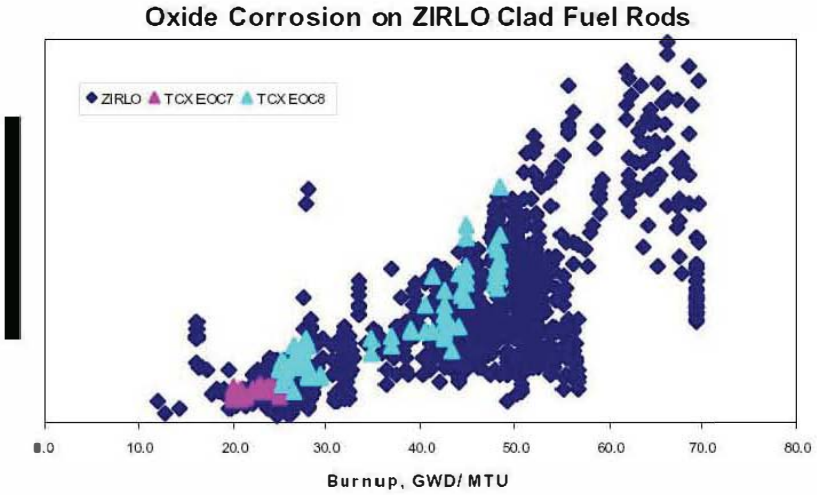

Figure 2-12: Measured Rod Oxide Thickness vs. Burn-up for Comanche Peak Unit 2 Cycle 7 and Cycle 8 Fuel against the Overall *ZIRLO*™ Database (Iyer et al., 2006(b)).

2.1.7 BWR Coolant Purification

The *BWR* primary coolant system is significantly more impurity prone than the *PWR* system, as the coolant passes through a longer, more complex circuit contacting a large variety of materials, potentially leaking seals, while the coolant changes temperatures, pressures and phases. As a result the coolant purification systems and their operation have a high priority in order to maintain the reliable performance of the circuit structural materials, assure fuel reliability and achieve dose reduction goals. Two noteworthy developments reported recently are summarized here.

A study sponsored by EPRI evaluated the condensate polishing practices of 39 BWRs in order to identify the parameters that best help achieve the above goals (Tran, 2006), specifically the iron (Fe), copper Cu) and sulfate (SO_4) control and the potential effects of power uprates on polisher operations. The effectiveness of three types of polishers were compared: (1) deep bed demineralizers most efficient for removing ionic impurities, (2) filter demineralizers most efficient for removing particulates and (3) filter demineralizers as "prefilters" followed by deep bed demineralizers. The most efficient in all cases, not surprisingly, were the combined filter+deep bed demineralizers. *The true efficiency of the filters should be measured by the difference in the input and output of the impurities, data not provided in this paper, which presumably is available in the original report.*

The filter+deep bed combination was able to reduce Fe content in the feedwater to <1ppb (Figure 2-13). The source of the Fe is primarily corrosion of carbon steel feedwater piping. The general reduction of feedwater Fe over the years:

- Reduces the amount of tenacious zinc ferrite crud deposits on the fuel that can accompany Zn injection,
- Reduces the amount of iron oxide crud on the fuel,
- Reduces the amount of costly depleted Zn needed for Zn injection.

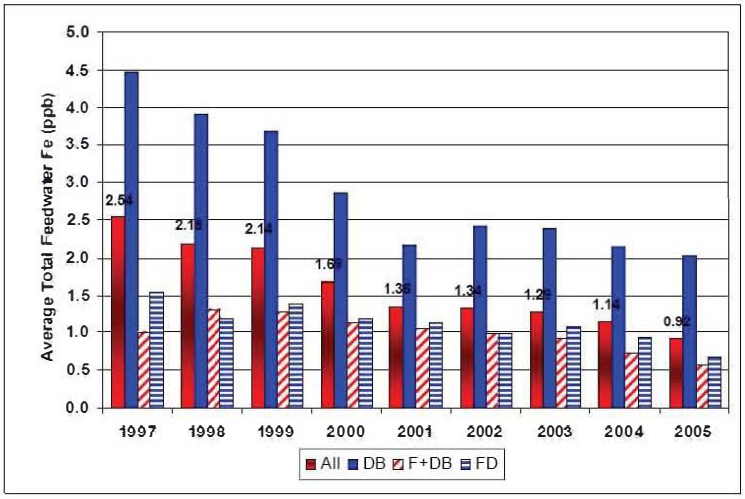

Figure 2-13: *BWR* Feedwater Iron Travel from 1997-2005 for 39 *BWR*s by Condensate Polishing System (Tran, 2006).

Reduction of SO_4 is also most efficient with the dual filter+bed demineralizer system (Figure 2-14). The source of the sulfate is from the decomposition of the cation resins in the polisher. Some of the sulfur species react and tend to foul the anion resins and one of the remedies has been to put a layer of anion resins at the bottom of the deep bed demineralizer to react with the sulfur species prior to the exit. The industry goal is to reduce SO_4 <2ppb to help mitigate *IGSCC* of the stainless steel structural components.

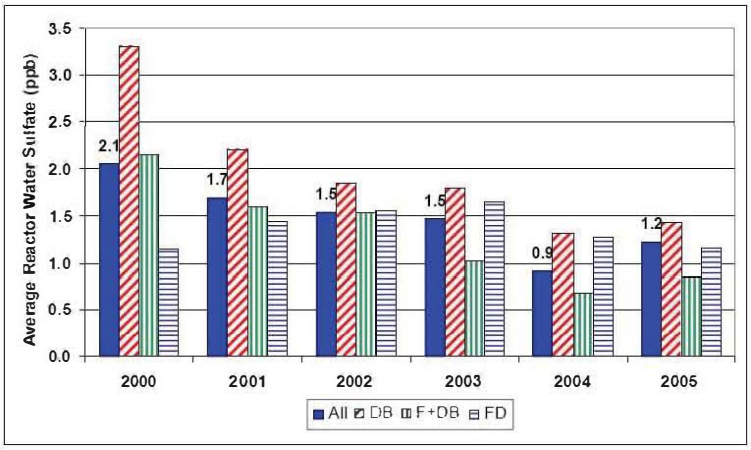

Figure 2-14: 2000-2005 Average Reactor Water Sulfate Differentiated by Condensate Polisher Type (Tran, 2006).

There are still 10 plants in the US with a significant Cu source from the main condenser and some have difficulties attaining the industry goal of < 0.05 ppb. The effectiveness of the dual demineralizer system is shown on Figure 2-15. Control of Cu is needed to avoid high density crud formation on the fuel (*CILC*). The presence of Cu also is counteractive in the reduction of the electrochemical potential (*ECP*) by *HWC* or *NMCA* requiring either one to inject more hydrogen for attaining the goal *ECP*.

3 ALLOY SYSTEMS (BRIAN COX)

New work on this topic remains minimal. However there are four papers published within the past year that warrants discussion. Pilloud et al., 2005, studied the formation of omega-phase in zirconium films sputtered onto steel, glass and silicon substrates. The effect of the substrate, interlayer and the compressive stress in the films on the formation of the omega-phase were investigated. The zirconium films were deposited by D.C. magnetron sputtering in the static mode using a 99.999% pure Zr target with 99.9999% pure argon as the sputtering gas. Initial vacuum pressure was $<10^4$ Pa. Substrates were either (100) Si; glass; or polished 32 CrMoV13 steel. Substrates were ultrasonically cleaned for 10 min. in acetone followed by 10 min. in ethanol. Some steel substrates were covered with interlayers of either: Cu; Cr; Ag; Fe; Mo or ZnN. Further experimental details are presented in the paper. During magnetron sputtering the bias-voltage induces low energy ion bombardment of the growing film. This generates compressive stresses in most films and leads to nucleation of non-equilibrium structures. However, this effect of the bias-voltage makes only a minor contribution to the formation of omega-phase, because this is also generated in the absence of a bias-voltage. Thus the substrate's nature is the primary cause of omega-phase formation. However, earlier work by Stauder & Frantz, 1991, did show a major effect of bias-voltage. Variability in the compressive stress generated seems to be the primary cause of these differences. This is related to the grain sizes of the alpha and omega that are achieved, Table 3-1. Grain size ratios greater than 4 appear to be necessary and this eliminates an α to ω transformation after film formation as the mechanism. Specific elements in the substrate seem to be of most importance. Of the elements tested Mo seems to be the most important of the substrate (or interlayer) elements generating two-phase $\alpha + \omega$ films, while Cr in the substrate produces entirely ω–films, Figure 3-1.

Table 3-1: Grain sizes and lattice parameters of α- and ω-phase in sputtered Zr films deposited on steel substrate.

V_b (V)	α-Phase			ω-Phase		Φ_ω/Φ_α
	Φ_α (nm)	a_α (nm)	c_α (nm)	Φ_ω (nm)	c_ω (nm)	
0	33	0.3226	0.5137	264.4	0.3138	8.0
−80	28.5	0.3247	0.5196	195.1	0.3141	6.8
−100	21.7	0.3243	0.5197	248.3	0.3144	11.4
−120	24.3	0.3244	0.5195	195.1	0.3150	8.0

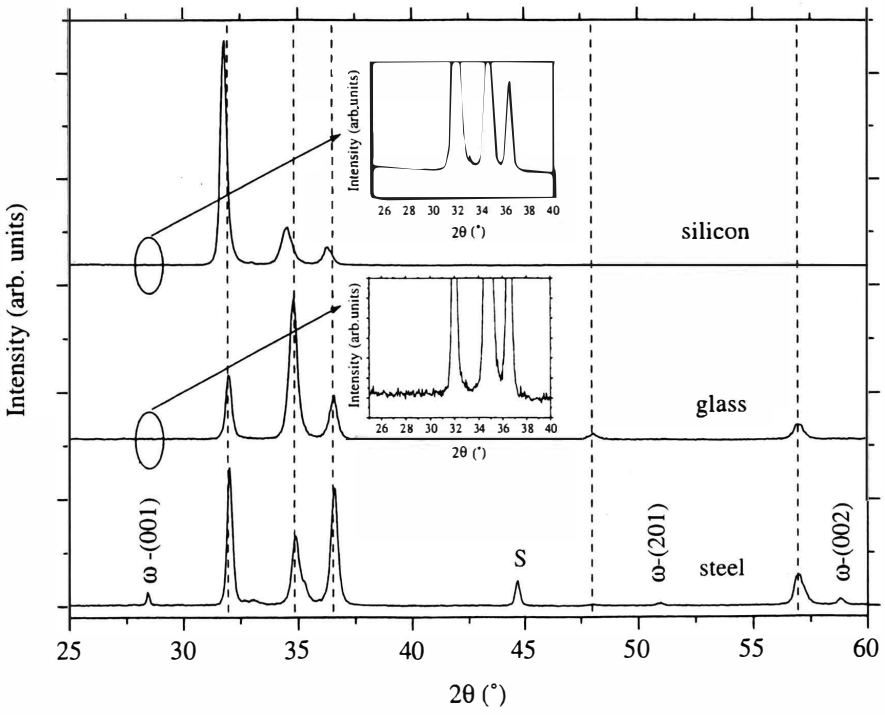

Figure 3-1: XRD patterns for unbiased Zr films deposited on steel, glass and silicon substrates (dashed lines relate to α-Zr and S label corresponds to the substrate peak). For glass and silicon substrates, an inset has been added to clearly show that there is no ω-phase diffraction peak at 20 close to 28.5°, Pillowed et al., 2005.

Kim et al., 2005(d) report some new work on the α/α+β/β transformation temperatures; the solubility limits of Nb; and the monotectoid temperature in the Zr/Nb binary system. They used material with 1400 ppm oxygen and 700 ppm Fe to distinguish their results from the early phase-diagram study of Lundin & Cox, 1962. Kim et al. annealed 2% Nb alloy specimens at 580 and 590°C, followed the disappearance of the β-Nb phase, Figure 3-2 and claimed a monotectoid temperature of 585°C, compared with the Lundin & Cox value of 620°C, Figure 3-3 and Figure 3-4. They offer no explanation for why the monotectoid temperature should be lower in their alloy than in the high purity alloy (< 100 ppm O) used by Lundin & Cox. Oxygen is an α-stabiliser and should increase the monotectoid temperature (if anything), and although Fe is a β-stabiliser, its solubility in Zr at these temperatures (~100 ppm) is too low to produce an observable shift in the monotectoid temperature. To justify their results they misquote the work of Toffolon et al., 2002, claiming that these authors obtained a value of 600 $\pm$ 5°C "which was only slightly different" from their result. In fact Toffolon et al. obtained a value of 630°C and showed that increasing the oxygen content resulted in only a small increase in the monotectoid temperature, Figure 3-5 and Figure 3-6 and that this temperature extrapolated to 620°C at zero oxygen content (identical with the Lundin & Cox value at ~100 ppm O).

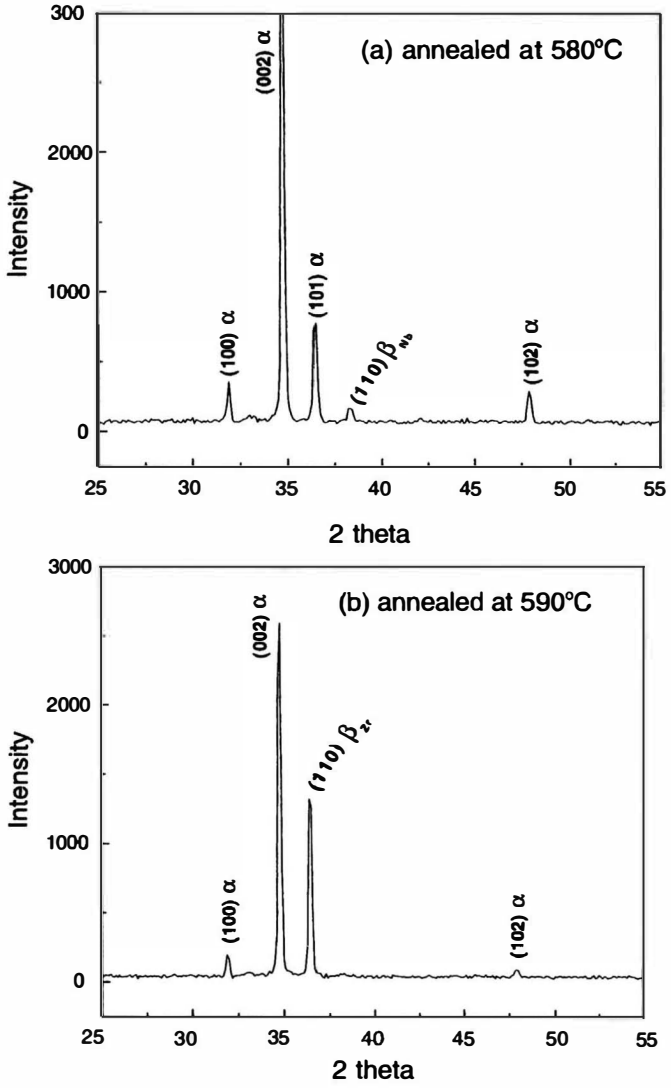

Figure 3-2: XRD spectra of Zr-2.0Nb alloys containing 1400 ppm O and 700 ppm Fe annealed at (a) 580°C and (b) 590°C for 3 months, Kim et al., 2005(d).

4 ZIRCONIUM ALLOY MANUFACTURING (GEORGE SABOL)

4.1 INTRODUCTION (GEORGE SABOL, BRIAN COX AND PETER RUDLING)

The material performance in-reactor is a function of the reactor environment as well as the material microstructure. The microstructure depends on the chemical composition and the manufacturing process of the alloy.

Figure 5-13 gives an overview of the manufacture of zirconium alloy strip and tube materials that are used to manufacture fuel cladding, guide tubes (*GT*) and grids for *PWR*s, and fuel cladding, water rods, channels and grids for *BWR*s.

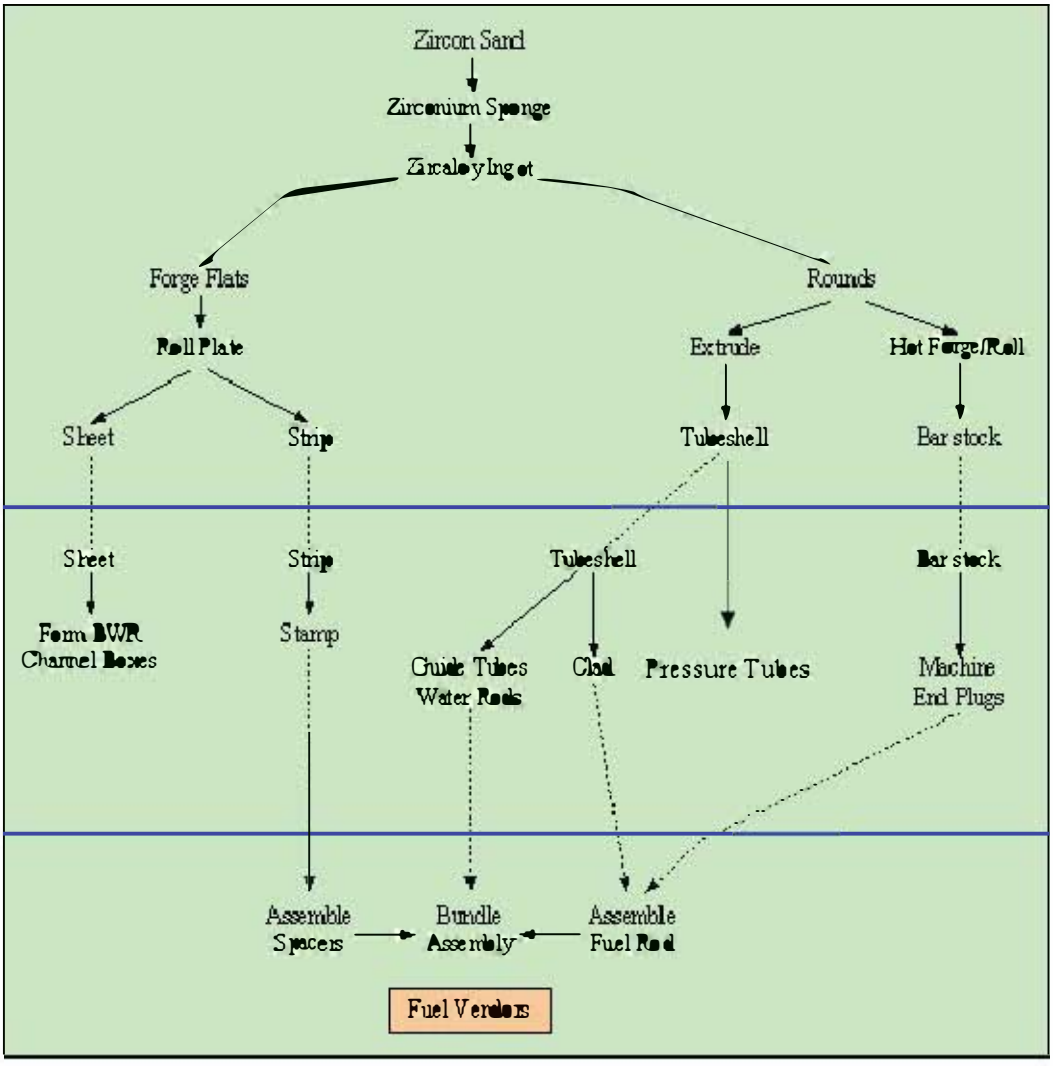

Figure 4-1: Zircaloy Production Outline.

The manufacturing process of different light water reactor (*LWR*) zirconium alloy products may be divided into three steps: 1) production of Zr raw material, 2) melting and primary processing (hot deformation), and 3) final product (tube, strip/sheet, bar) fabrication.

Nearly all the zirconium metal is extracted from zircon, Zr-Hf SiO_4, which is found in beach sand, with the richest deposits in Australia. The zirconium to hafnium ratio in zircon is about 50/1, but since Hf has a very large thermal neutron cross section, it is crucial that as much Hf as possible is separated from zirconium during the manufacturing process.

The current dominant process to produce Zr metal is the Kroll process, reduction of zirconium tetrachloride with molten magnesium, which results in zirconium sponge. Zirconium sponge, recycle material from earlier manufacturing, and alloying elements are assembled into an electrode that is arc-melted in a consumable electrode process in a vacuum. The resulting ingot is remelted, usually twice, to increase the homogeneous distribution of the alloying elements.

The ingots are converted to products according to a sequence of plastic deformations to final shape. Deformation processing is divided into hot and cold forming processes. The temperatures in the former are high enough to cause dynamic recrystallization, whereas, the latter processes are done at such a low temperature, usually room temperature, that recrystallization does not occur during deformation. Intermediate recrystallization anneals are performed to restore the ductility after cold deformation.

For round products the ingots are hot forged into round billets, called "logs", by use of a hydraulic press or by rotary forging, the latter giving a more homogeneous plastic deformation. The logs may be further processed directly, or cut into shorter segments for further processing.

The next step in manufacturing is the beta-heat treatment and quenching process. Alloy billets are heated into the high temperature β-phase region (~1100°C) to dissolve the phases formed during the hot working and to homogenize the product by decreasing the microsegregation of the alloying elements. Rapid cooling by water quenching is used to maintain uniformity of alloy distribution by avoiding constitutional segregation as the cooling proceeds through the two-phase (α + β) region and to suppress precipitation of large second phase particles (*SPP*s).

If a "log" was beta-quenched, it is then cut up in smaller sized billets for subsequent processing to tube shells and pressure tubes. Alternately, the "log" may be cut into billets and then β quenched. After the β-quench the solid billets are then pierced to get a central hole (the pierced billet can also be beta-quenched resulting in faster cooling rate). Then the billet with a pierced hole is machined to remove the oxide scale and the surface beneath the oxide that may be contaminated from the earlier processing operations.

For extrusion, the billets are heated to the extrusion temperature (600-750°C), put into the extrusion press, and extruded to tube hollows.

Processing of the extrusions to cladding or guide tubes proceeds in several steps by cold pilgering, also called rocking, or tube reducing. In most cases, three to four reduction passes are required to reduce the extrusion to the final tubing size. After each reduction pass, the tubes must be cleaned and vacuum annealed to prepare them for the next cold reduction pass. The annealing treatments promote recystallization and soften the material. For pressure tubes the extrusions are typically cold drawn to size, with or without an intermediate anneal.

For Zircaloy-2 and -4 used in *BWR*s and *PWR*s the selection of the intermediate annealing temperatures is dictated by the integrated thermal exposure of the material after the β-quench. With increasing thermal exposure, the excess iron, chromium, and nickel (for Zircaloy-2) above the solubility limit are precipitated as second phase intermetallic particles of $Zr(Fe,Cr)_2$ and $Zr_2(Fe,Ni)$. The extent of precipitation and precipitate size increases with thermal exposure. As it has been found that there is a direct relationship between the integrated thermal exposure and corrosion resistance, the thermal exposure is monitored by an "Annealing" parameter, A, which is a measure of the total heat input after the last beta-quenching according to:

$$A = \Sigma t_i \exp\left(-Q / RT_i\right)$$

where,

t_i (in hours) and T_i (in Kelvin) are the time and temperature of annealing step i

Q is an activation energy, and,

R is the gas constant.

Different activation energies have been used, and values in the range 63,000 to 80,000 cal/mole/K have shown good correlation of thermal exposure with corrosion resistance, Andersson et al., 1987, and Garzarolli et al., 1989(a). As thermal exposure leads to precipitation and growth of *SPP*s, there is also a relation between the cumulative thermal exposure and particle size, and quantitative relationships have been described by use of a Particle Growth Parameter (*PGP*), Steinber & Pohlmeyer, 1997, and by a Second Order Cumulative Annealing Parameter (*SOCAP*), Groß & Wadier, 1990. The *PGP* and *SOCAP* relations may offer advantages when accounting for short annealing times, e.g. strips produced by continuous rolling/annealing.

The Zircaloys are usually used in the recrystallized condition in both *PWR*s and BRWs. The exception is fuel cladding in *PWR*s, which is used in the cold-worked-and-stress-relief-annealed (*CWSRA*) or partially recrystallized conditions. Use of *RXA* material for grids and guide tubes in *PWR*s is to ensure enough ductility during manufacturing of the fuel assembly structure, which normally involves heavy plastic deformation of the guide tube to interlock it to the spacer grids. *RXA* material also provides reduced irradiation growth and creep compared to material in the *CWSRA* condition, an advantage for dimensional stability of the assembly.

5 MECHANICAL PROPERTIES (RON ADAMSON AND BRIAN COX)

5.1 INTRODUCTION (RON ADAMSON)

The mechanical properties of essentially two different components are normally treated in this section. First, the *LWR* fuel assembly and, second, the *Pressure tubes*` in *CANDU* reactors. The difference between these two components is that the fuel is reloaded after some time in-reactor while the *Pressure tube* is a part of the reactor design and must consequently perform satisfactorily during the lifetime of the reactor.

Delayed hydride cracking, *DHC*, is a failure mechanism that may limit the lifetime of *CANDU* and *RBMK* pressure tubes, and this mechanism is therefore treated in the pressure tube section. Delayed Hydride Cracking, *DHC*, is a fracture mechanism that may result in pressure tube failures as well as degradation of failed *LWR* fuel. A better understanding of the relation of the *DHC* mechanism to the material properties may e.g. assist the fuel vendors to develop products with enhanced resistance towards *DHC*.

In a *CANDU* reactor the cold-worked Zr-2.5Nb pressure tubes operate at temperatures between about 250 and 310°C and at coolant pressures of about 10 MPa corresponding to hoop stresses of about 130 MPa. The maximum flux of fast neutrons from the fuel is about $4\ 10^{17}$ n $m^{-2}s^{-1}$.

The pressure tubes used in a *CANDU* reactor are made from Zr-2.5Nb. The tubes are extruded at 815°C cold worked 27% and stress relieved at 400C for 24 hours, resulting in a structure consisting of elongated grains of hexagonal-close-packed (*HCP*) α-Zr, partially surrounded by a thin network of filaments of body-centered-cubic β-Zr. These β-Zr filaments are metastable and initially contain about 20% Nb. The stress-relief treatment results in partial decomposition of the β-Zr filaments with the formation of hexagonal-close-packed ω-phase particles that are low in Nb, surrounded by an Nb-enriched β-Zr matrix. The hcp α-Zr grains are oriented with their unique c-axes aligned in the radial-transverse plane, mostly tilted towards the transverse direction.

The mechanical properties of the *LWR* fuel assembly is crucial for its satisfactory performance in-reactor. *Standard Review Plan, SRP*, section 4.2, lists different mechanical failure modes of the *LWR* fuel components and also the corresponding design criterion to ensure that the fuel assembly behavior is satisfactory. These design criteria are set to ensure that:

- The fuel assembly will not fail during normal operation (class I) and anticipated operational occurrences (class II). *Failing* in this sense has a broader meaning, namely that the fuel rod may not be breached and that the dimensional changes of the assembly during irradiation must be limited. The latter requirement is to ensure that control rods can be inserted and that the fuel can be handled during shutdown. Also the *BWR* fuel outer channel cross section must not have increased to such an extent that it is impossible to pass it through the upper core grid during reloading.

- The fuel remains coolable during an accident (class III and IV). Class IV design basis accidents are *LOCA, RIA* and earthquake. During class III and IV situations limited fuel failures are however accepted. Another criterion that must be fulfilled in these situations is that it should be possible to insert the control rods.

- During class I and II operation, the following mechanical *failure* mechanisms and corresponding design criterions for the fuel assembly, including its components, are listed in *SRP* section 4.2:

- Plastic deformation – the component is regarded as *failed* if it is plastically deformed and the appropriate criterion is that the stresses must be lower than the yield stress. *SRP* section 4.2 also state what type of methodology should be used when calculating these stresses. In these calculations the stress in the assembly location subjected to maximum stresses is calculated. In calculating this stress, all types of stresses are taken into account, such as welding residual stress, thermal stress, stress imposed by rod-system differential pressure, etc. It is interesting to note that the criterion on maximum allowable oxide thickness on fuel rods is related to this criterion. If the oxide thickness becomes too large in a *PWR*, the oxide thickness will increase the cladding temperature due to its lower thermal conductivity and would then increase corrosion rate. The oxide thickness would increase further, raising the clad temperature and corrosion rate, resulting in thermal feedback. Since increasing temperature decreases the yield strength of the material, the material would eventually mechanically fail, i.e., plastically deform, provided that the cladding stresses are large enough.

- Excessive creep deformation that could either result in creep fracture or too large plastic deformations that could e.g. lead to *dryout* due to excessive outward creep of the fuel cladding diameter that would limit coolant flow. Creep occurs at a stress level lower than the yield stress. The corresponding criterion is very general and just specifies that the creep deformation must be limited.

- Fatigue failure – Most fuel assembly components are subjected to fatigue stresses and *SRP* section 4.2 provides the maximum allowable fatigue stress level.

- *PCI* – The criterion to eliminate this type of failure is by limiting the elastic and uniform plastic deformation in the cladding circumference during a class I and II transient to 1%. This value is of course not sufficient to ensure that *PCI* failures do not occur. However, the fuel vendors are still designing their fuel so this 1% limit is achieved in their design.

- Hydride embrittlement – The criterion just mentions that the hydrogen content in the material must be limited so the fuel assembly component will not fail.

During accident conditions such as *LOCA* and *RIA*, the mechanical performance of the fuel cladding is crucial to meet the objective that the fuel must remain coolable during these types of accidents. In both situations, it is important that the fuel cladding may not fail in a brittle fashion during the reflooding[1] phase during *LOCA* and due to *PCMI*[2] during a *RIA* transient.

Fuel vendors have developed codes to model the fuel assembly mechanical performance during class I, II, III and IV situations. To be able to do the modelling correctly, data on mechanical performance of the fuel assembly must exist. The data are generated in two types of tests, either separate effect tests or integral tests. The former test studies only the impact of one parameter at a time on the mechanical performance, see e.g. Adamson & Rudling, 2001, This could e.g. be the impact of hydrogen content on ductility. The data from these separate effect tests are then used by the fuel vendor to develop adequate models in their fuel performance codes. To then verify that the code comes up with the correct prediction on fuel assembly mechanical performance e.g. during a *LOCA*, the code predictions are benchmarked towards integral tests. In the integral test, the fuel assembly design and environment is as similar as possible as is existing in the situation that is simulated in the test, e.g. a *LOCA*.

5.1.1 Summary from *ZIRAT* 10 (Ron Adamson)

Review of the late-2004 to late-2005 literature pertinent to the mechanical properties of zirconium alloys has resulted in the following observations:

- There was an insufficient number of papers to allow proper review of stress corrosion cracking and delayed hydrogen cracking.
- Formation of "radial hydrides", that is, with the long axis of the hydride parallel to the radial direction of clad tubing, is being intensely studied. The application is to *RIA* and fuel storage issues.
- Reorientation of hydrides from the circumferential to the radial direction can occur under a hoop stress of above 80 MPa (11,360 psi) at 400°C (673K), where the solubility of H is about 200 ppm.
- For unirradiated Zircaloy-2, Zircaloy-4 or ZrNbSnFe alloys.
- Based on very scant data, for irradiated Zircaloy-4, where the H solubility may be >200 ppm.
- The compression yield stress for a typical delta hydride decreases sharply in the 20-150°C (293-423K) temperature range, and then levels out to as high as 400°C (673K).

---

[1] This is the last phase during a *LOCA* situation when the core is reflooded with water that cools the fuel cladding surface imposing very large thermal stresses that may fracture the fuel cladding.
[2] Pellet Cladding Mechanical Interaction, i.e., interaction without the influence of iodine (that would instead result in *PCI* (Pellet Cladding Interaction).

6 DIMENSIONAL STABILITY (RON ADAMSON)

6.1 INTRODUCTION

One of the most unique aspects of material behavior in a nuclear power plant is the effect of radiation (mainly neutrons) on the dimensional stability of reactor components. In fast breeder reactors the Fe and Ni-based alloys creep and swell, that is, they change dimensions in response to a stress and change their volume in response to radiation damage. In light water reactors, zirconium alloy structural components creep, do not swell, but do change their dimensions through the approximately constant volume process called irradiation growth. Radiation effects are not unexpected since during the lifetime of a typical component every atom is displaced from its normal lattice position at least 20 times. With the possible exception of elastic properties like Young's Modulus, the properties needed for reliable fuel assembly performance are affected by irradiation. A straightforward summary of such effects is given by Adamson and Cox, "Impact of Irradiation on Material Performance", *ZIRAT* 10 Special Topics Report, 2005.

Practical effects of dimensional instabilities are well known and it is rare that a technical conference in the reactor performance field does not include discussions on the topic. Because of the difference in pressure inside and outside the fuel rod, cladding creeps down on the fuel early in life, and then creeps out again later in life as the fuel begins to swell. A major issue is to have creep strength sufficient to resist outward movement of the cladding if fission gas pressure becomes high at high burnups. *PWR* guide tubes can creep downward or laterally due to forces imposed by fuel assembly hold down forces or cross flow hydraulic forces – both leading to assembly bow which can interfere with smooth control rod motion. *BWR* channels can creep out or budge in response to differential water pressures across the channel wall, again leading toward control blade interference. Fuel rods, water rods or boxes, guide tubes, and tie rods can lengthen, possibly leading to bowing problems. (For calibration, a recrystallized (*RX* or *RXA*) Zircaloy water rod or guide tube could lengthen due to irradiation growth more than 2 cm. during service; a cold worked/stress relieved (*SRA*) component could lengthen more than 6 cm.) Even *RX* spacer/grids could widen enough due to irradiation growth (if texture or heat treatment was not optimized) to cause uncomfortable interference with the channel.

In addition, corrosion leading to hydrogen absorption in Zircaloy can contribute to component dimensional instability due, at least in part, to the fact that the volume of zirconium hydride is about 16% larger than zirconium. The above discussion leads to the concept that understanding the mechanisms of dimensional instability in the aggressive environment of the nuclear core is important for more than just academic reasons. Reliability of materials and structure performance can depend on such understanding.

A comprehensive review of dimensional stability has been given in the *ZIRAT* 7 Special Topical Report – "Dimensional Stability of Zirconium Alloys"; Adamson & Rudling, 2002. The sources of dimensional changes of reactor components (in addition to changes caused by conventional thermal expansion and contraction) are: irradiation growth, irradiation creep, thermal creep, stress relaxation (which is a combination of thermal and irradiation creep), and hydrogen and hydride formation.

Irradiation effects are primarily related to the flow of irradiation-produced point defects to sinks such as grain boundaries, deformation-produced dislocations, irradiation produced dislocation loops, and alloying and impurity element complexes. In zirconium alloys, crystallographic and diffusional anisotropy are key elements in producing dimensional changes.

In the past, hydrogen effects have been considered to be additive to and independent of irradiation; however, recent data have brought this assumption into question. It is certain that corrosion-produced hydrogen does cause significant dimensional changes simply due to the 16-17% difference in density between zirconium hydride and zirconium. A length change of on the order of 0.25% can be induced by 1000 ppm hydrogen in an unirradiated material. Whether or not the presence of hydrides contributes to the mechanisms of irradiation creep and growth is yet to be determined.

Fuel rod diametral changes are caused by stress dependent creep processes. Fuel rod length changes are caused by several phenomena:

- Stress free axial elongation due to irradiation growth.
- Anisotropic creep (before pellet/cladding contact) due to external reactor system pressure. Because of the tubing texture, axial elongation results from creep down of the cladding diameter; however for heavily cold worked material, it has been reported that some shrinkage may occur. In a non-textured material such as stainless steel, creep down of the cladding would only result in an increase in cladding thickness, with no change in length.
- Creep due to pellet-cladding mechanical interaction (*PCMI*) after hard contact between the cladding and fuel. This occurs in mid-life, depending on the cladding creep properties and the stability of the fuel.
- Hydriding of the cladding due to corrosion.

Bow of a component such as a *BWR* channel or *PWR* control rod assembly can occur if one side of the component changes length more than the other side. Such differential length changes occur due to differential stress and creep, relaxation of differential residual stresses, or differential growth due to differences in flux-induced fluence, texture, material cold work, and hydrogen content (and, although not usually present, differences in temperature or alloying content.

Review of the mid-2004 through late 2005 literature on dimensional stability was reported in the *ZIRAT* 10 Annual report, Adamson et al., 2005. Reported highlights include:

- Several data sets indicate that microchemistry strongly influences growth and creep.
- Available microstructural exams have not been able to determine the critical parameters which cause <c> component dislocation loop initiation. Thus, there is still uncertainty about the source of different behaviors of M5 and E110.

- E110 has been shown to respond in a "normal" way to texture effects.
- The possible effect of hydride or hydrogen on the stress-free growth mechanism has not yet been explained or discounted.
- Rapid grid-spring force relaxation was shown to occur early in bundle life, with some residual spring force remaining at end of life.
- Hydride volume swelling strongly influences grid/spacer envelope dimensions, but does not account for the total observed changes.
- Only small differences exist in fuel length change for *RXA* cladding in different bundle designs and duty histories.
- Good evidence exists for the approximately constant volume assumption for irradiation growth in Zr2.5Nb.

The current *ZIRAT* 11 Annual Report reviews the literature from late 2005 to late 2006.

6.2 BOOK REVIEW

Zirconium in the Nuclear Industry, 14th International Symposium, *ASTM* STP 1467, Peter Rudling and Bruce Kammenzind, editors, *ASTM* International, West Conshohocken, PA, 2005. This book, issued in 2006, contains the final version of papers presented at the Stockholm meeting of June 2004. Most of the papers were reviewed in the *ZIRAT* 10 Annual Report, so just brief comments are given here to allow the reader to easily look up the papers in the book. All the papers were also published in Journal of *ASTM* International, which is the official reference for the paper. In our review here, the page number in the *ASTM* 1467 book is given in parenthesis.

- "Destruction of Crystallographic Texture in Zirconium Alloy Tubes", Grytsyna et al., 2005 (page 305). This paper describes a fabrication technique to produce fine-grained random texture components of Zr 2.5 Nb. Data is given showing near zero irradiation growth for the specially fabricated alloy.
- "Modeling of the Simultaneous Evolution of Vacancy and Interstitial loops in hcp Metals Under Irradiation", Dubinko et al., 2006 (page 157). To understand irradiation growth, creep and hardening it is necessary to understand details of the formation of dislocation loops in zirconium alloys. This paper produces a complicated model for formation, and outlines parameters which are needed to make the model more reliable.
- "The Effect of Beta-Quenching in Final Dimension on the Irradiation Growth of Tubes and Channels", Dahlbäck et al., 2005 (page 276). This paper describes a beta-quench-plus-anneal fabrication method to produce channel and water rod components. Ideally, ransom texture is produced which would promote very low growth and bar of channels while maintaining good corrosion resistance. Data indicate good results, at least to moderate burnup.

7 CORROSION & HYDROGEN UPTAKE (BRIAN COX, FRIEDRICH GARZAROLLI)

There has been a surprising decline this year in the number of papers published in the areas of stabilised ZrO_2 properties and the electrical properties of ZrO_2 in electronic devices. This suggests that nanomaterials studies may be moving into other areas.

These has been no publication yet of the proceedings of the *IAEA* Technical Committee Meeting on "Behaviour of High Corrosion Resistance Zr- Based Alloys" (Buenos Aires, Arg., 24-28 Oct. 2005) either in the form of a C. D or an *IAEA*-TECDOC. The discussion of results presented at this meeting will, therefore be based on preprints obtained from the presenters at (or after) the meeting. Readers should be aware that the possibility of some changes being made to these texts remains until the final version of the proceedings is published.

7.1 ZRO$_2$ STUDIES AND THIN FILMS (BRIAN COX)

Choi et al., 2005 present some results on the effects of fabrication variables on the mechanical properties of zirconia thermal barrier coatings. They applied annealing times of o-500 hr. at 1316°C in air to coatings of ZrO_2 – 8wt% Y_zO_3 plasma-sprayed on a graphite base (which was removed before testing). The specimens were tested for 4-point flexure strength; fracture toughness (modes I and II; stress/strain in compression; density and Vickers micro hardness; and thermal conductivity by laser). All test at ambient temperature. The collected data for all tests are combined in Figure 7-1. Only the fracture toughness, Figure 7-2 and increase in monoclinic ZrO_2 content, Figure 7-3, remainder was t-ZrO_2, are presented separately.

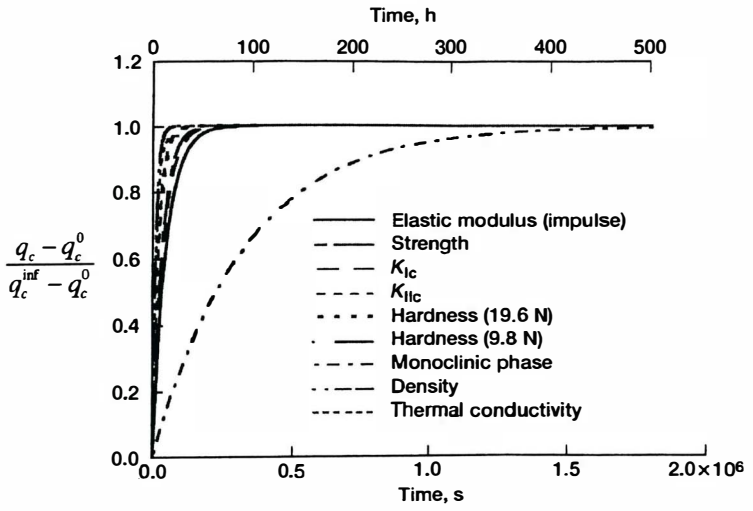

Figure 7-1: Results of application of model (Eq. (7)) to various property values determined for plasma-sprayed ZrO_2-8 wt% Y_2O_3 thermal barrier coatings annealed at 1316°C in air, Choi et al., 2005.

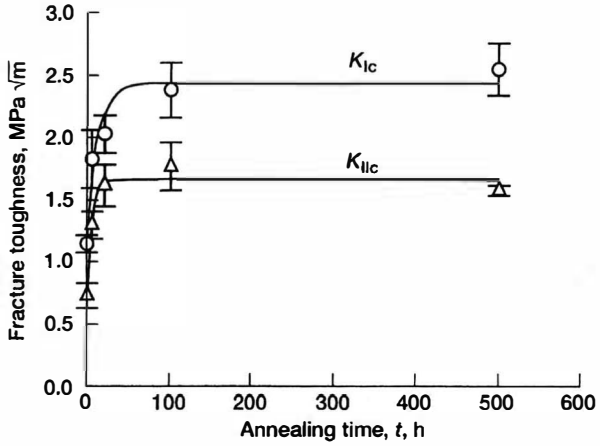

Figure 7-2: Modes I and II fracture toughness (K_{1C} and K_{11C}) as a function of annealing time for plasma-sprayed ZrO_2-8 wt% Y_2O_3 thermal barrier coatings annealed at 1316°C in air. Error bars indicate ±1.0 standard deviation, Choi et al., 2005.

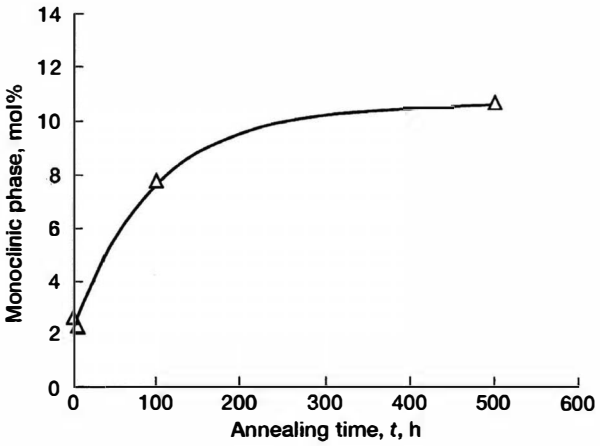

Figure 7-3: Percent of monoclinic phase as a function of annealing time for plasma-sprayed ZrO_2-8 wt% Y_2O_3 thermal barrier coatings annealed at 1316°C in air, Choi et al., 2005.

Lee et al., 2005(a) presented results on the effects of nitrogen diffused into the surface of yttria (2%) stabilised tetragonal zirconia polycrystals in contact with ZrN at ≥ 1500°C. The nitrided layers consisted of a nitrogen-rich cubic matrix with nitrogen-poor t-ZrO_2 crystals precipitated throughout. The stabilisation of cubic zirconia is a result of the anionic vacancies created and N is just as effective a stabiliser as Mg, Ca or Y. The effect of nitrogen on the zirconia ionic conductivity was measured by impedance spectroscopy. Gold was evaporated onto the polished surfaces in a lattice of small (10 μmdia) microelectrode arrays. The ionic conductivity tests were conducted at 300 and 400°C. The regions in which nitrogen was diffused (on both faces of the specimens) developed columnar cubic ZrO_2, Figure 7-4. The total specimen thickness was 2 mm and only a small region (250 mm) in the centre of each specimen seems to have been free of nitrogen induced columnar grains but was not free of nitrogen and appeared to have developed micro porosity. With ZrN diffused in from one side only, Figure 7-5 the columnar grains were more clearly delineated. No d.c. conductivity measurements were made. However, the observation of a stimulation of columnar crystallite growth in zirconia layers may have relevance when effects of nitrogen in Zr on oxide growth are considered.

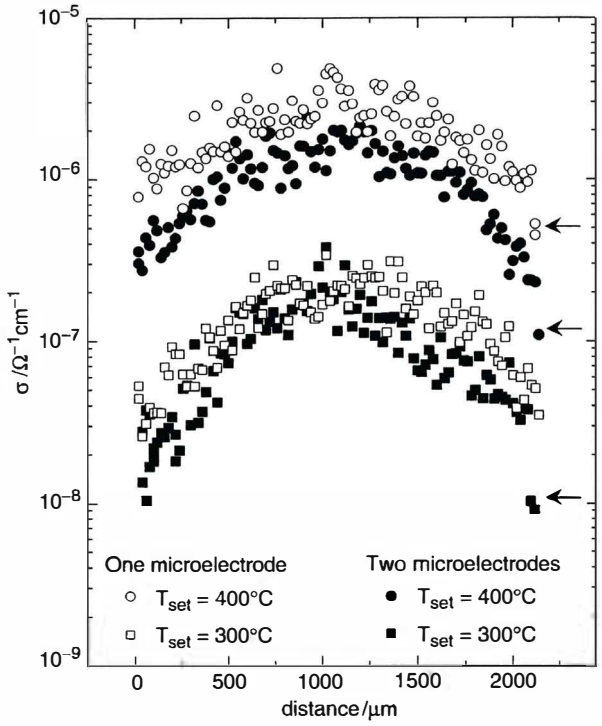

Figure 7-4: Conductivity profiles of a nitrogen-stabilized zirconia specimen treated at 1700°C for 4h (micrograph on top). Temperatures of the hot plates (T_{set}) were 300°C (squares) and 400°C (circles), respectively. Open symbols represent measurements between one microelectrode on top and the counterelectrode at the bottom of the specimen, and closed symbols indicate measurements using two top microelectrodes, Lee et al., 2005(a).

8 EFFECTS OF WATER CHEMISTRY

8.1 PWR WATER CHEMISTRY (R●LF RIESS)

8.1.1 Introduction

The Primary Coolant serves as a moderator and is the medium for transporting heat from the core to the steam generators. Hence, it must not endanger plant operation by the corrosion of materials and consequences thereof. The task of water chemistry can be divided into the following main points.

- Metal release rates of the structural materials should be minimal.
- The occurrence of localized forms of corrosion should be counteracted.
- The transport and deposition of corrosion products must be influenced in such a manner, that contamination of the primary coolant system is kept low.
- The deposition of corrosion products on heat transfer surfaces, particularly on fuel assemblies, should be prevented as far as possible.
- Radiolytic formation of oxygen should be suppressed.
- The materials which are in contact with the primary coolant are:
- Austenitic stainless steels of components and piping of the primary system.
- Zirconium alloys for cladding of fuel assemblies.
- Incoloy 8●●, Inconel 69● TT or, Inconel 6●● MA or TT for steam generator tubes. Stainless steel tubing is used in *VVER SG*s.
- High alloy materials (ferritic stainless steels) of low surface area for internals of the primary system.

The water chemistry conditions applied to these materials must fulfil the above mentioned requirements. Thus the primary coolant of *PWR*s, which contains boric acid (9●●-18●● ppm B at *B●C*) as a neutron absorber, is chemically conditioned by the addition of isotopically pure lithium (Li- 7) hydroxide (2-5 ppm Li at *B●C*) as a non volatile pH-control agent and of hydrogen.

Recently, an increasing number of *PWR*s is adding Zinc (5-4● ppb) in order to (1) reduce plant activation by reducing the metal release and by replacing Cobalt isotopes in the oxide layer and (2) minimize the initiation of stress corrosion cracking of Inconel 6●● material.

In *VVER* plants NH_3 is added, which decays to H_2 by radiolysis. Instead of LiOH, KOH is added, so that the pH-control is accomplished by K + Li + Na (Li-7 is formed by the B-1● (n, α) Li -7 reaction) and NH_3. None of the *VVER* plants is adding Zinc like the *PWR*s.

8.1.1.1 Concerns regarding Fuel Elements

From today's perspective it is most important to evaluate the factors, which are of greatest concern for the fuel element corrosion and what are the driving forces (problems) for Water Chemistry in the last 1●- to 15 years.

These driving forces are moves to improve Plant Availability and Fuel Economics which can be characterized by:

- Changing to 18 and 24 month cycle
- Core up-rating
- Higher enrichment fuel, increased burn-up
- Low leakage cores combined with increased sub-cooled nucleate boiling.

These moves - based on operational experience - caused concerns over coolant additives and impurities because the fuel elements in the operating plants (specially in the US) experienced heavy crud deposition at positions where sub-cooled boiling created two negative effects, namely (1) accelerated corrosion effects and (2) Axial Offset Anomaly (*A●A*).

The corrective actions believed to be effective, are:

- Higher pH Primary Water Chemistry
- Zinc Addition

For the pH strategy it is believed to avoid in any case pH_T-values of < 6.9 by increasing the LiOH concentration above a long time valid value of 2-2.2 ppm Li. However, such Lithium increase may be a risk regarding the corrosion resistance of the Zirconium Alloys.

Specifically one environmental factor may be emphasized which is the corrosion product deposition on fuel surfaces, which can lead to increased cladding temperatures and increased corrosion rates. Such deposits have been identified as non-stoichiometric Ni-ferrites ($Ni_xFe_{3-x}O_4$), Ni oxide or metallic Nickel. Such crud deposition is occurring specifically at positions with sub-cooled boiling and may cause accelerated corrosion defects locally and axial power shift by boron precipitation (*A●A*).

Zinc addition may also lead to a more degrading crud at positions with high steaming rates. Thus, surveillance programs after introduction of Zinc are highly recommended, especially for *PWR*s with high duty cores. On the other hand, Zinc reduces the corrosion product release from system surfaces.

8.1.1.2 Higher pH Primary Water Chemistry; Lithium/B-Strategy

Historically, the solubility of magnetite was the basis for fixing a pH_T at 6.9 as an optimum. In addition, isotopically pure Lithium-7-hydroxide became the most suitable pH control agent to be used in the *PWR* Primary Coolant.

However, later on it was recognized, that the contribution of Nickel is much more important to the primary side corrosion product inventory than the iron. Further on it was found, that Nickel ferrite is a major constituent. Consequently the solubility behaviour of Nickel ferrite was investigated and it was found, that a pH of 7.4 should be the solubility minimum. However, a pH of 7.4 could not be adjusted at *BOC* since 2 or 2.2 ppm Lithium was at the upper specified limit in order to prevent Lithium induced corrosion of the fuel element cladding. As a consequence, the first two thirds of a cycle the 2 ppm were kept constant till reaching the pH of 7.4 and then Lithium/Boron ratio was adjusted to stay at 7.4 till end of the cycle.

In order to explain all the Li/B-ratio changes, it is convenient to use the information shown in Figure 8-1 for the US case by Turnage. Further details can be found in a review of the EPRI Water Chemistry Guidelines by Fruzzetti et al., 2004.

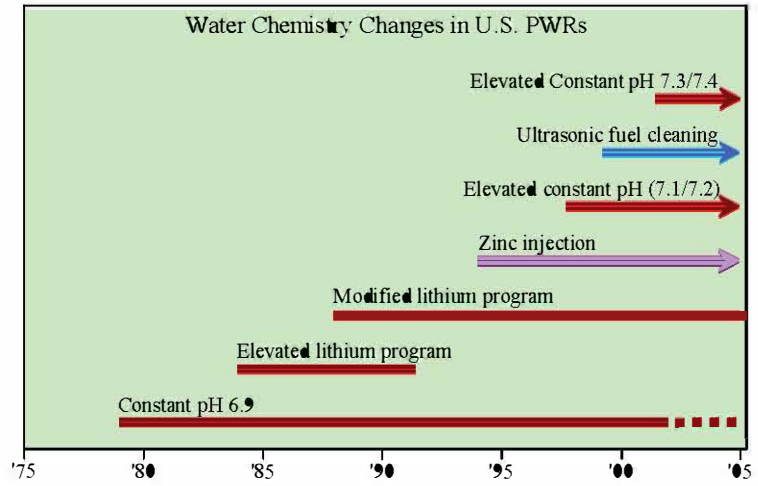

Figure 8-1: Water Chemistry Changes in U.S. *PWR*s, Turnage, 2004.

Regarding the application of all the Li/B-chemistries in operating *PWR*s there are major differences when applied in the various countries. These are discussed in detail in LCC-2 AR, Chapter 6.

The German *PWR*s for example are still operating today with the modified B/Li-program and therefore the specification, given by AREVA NP and VGB respectively, have an upper Lithium limit of 2.2 ppm. Only in very specific cases, utilities can apply Lithium values higher than 2.2 with the consent of the fuel manufacturer.

Bretelle et al., 2004 and Nordmann, 2005, described the actual situation in France regarding the optimum pH in the primary circuit of *PWR*s. According to their explanation, the $pH_{300\,^{\circ}C}$ of 7.2 $\pm$ 0.2 is applied because this value seems to be a good optimum for French *PWR*s based on the "DUO" experimentation which was performed for several cycles in Cattenom and based on the international experience. It should not be higher for materials reasons like stress corrosion cracking, particularly on Alloy 600 and it should not be lower, because of corrosion product transport and *AOA* (*CIPS*). A typical French primary water chemistry for older EDF-stations is shown in Figure 8-2.

9 PRIMARY FAILURE AND SECONDARY DEGRADATION –OPEN LITERATURE DATA (PETER RUDLING)

9.1 INTRODUCTION

9.1.1 Primary Failures

During reactor operation, the fuel rod may fail due to a primary cause such as fretting, pellet-cladding interaction (*PCI*), manufacturing defects, corrosion, etc., Table 9-1.

Table 9-1: Primary failure causes for *LWR* fuel during normal operation and anticipated operational occurrences.

Primary Failure Cause	Short Description
Excessive Corrosion	An accelerated corrosion process results in cladding perforation. This corrosion acceleration can be generated by e.g., *CRUD* deposition (*CILC*[11]), enhanced spacer shadow corrosion, *ESSC*,[12] (in *BWR*s), dry-out due to excessive fuel rod bowing.
Manufacturing defects	Non-through-wall cracks in the fuel cladding developed during the cladding manufacturing process. Defects in bottom and/or top end plug welds. Primary hydriding due to moisture in fuel pellets and or contamination of clad inner surface by moister or organics. Too large a gap between the fuel rod and the spacer grid supports (poor spacer grid manufacturing process) leading to excessive vibrations in *PWR* fuel causing fretting failures. Chipped pellets may result in *PCI* failures both in liner and non-liner fuel
PCI	Pellet Cladding Interaction—an iodine assisted stress corrosion cracking phenomenon that may result in fuel failures during rapid power increases in a fuel rod. There are three components that must occur simultaneously to induce *PCI* and they are: 1) tensile stresses—induced by the power ramp, 2) access to freshly released iodine-occurs during the power ramp, provided that the fuel pellet temperature becomes large enough and 3) a sensitised material—Zircaloy is normally sensitive enough for iodine stress-corrosion cracking even in an unirradiated state.
Cladding collapse	This failure mechanism occurred due to pellet densification. This failure mode has today been eliminated by fuel design changes and improved manufacturing control.
Fretting	This failure mode has occurred due to: Debris fretting in *BWR* and *PWR* Grid-rod fretting - Excessive vibrations in the *PWR* fuel rod causing fuel failures. This situation may occur for example due to different pressure drops in adjacent fuel assemblies causing cross-flow. Baffle jetting failures - Related to unexpectedly high coolant cross-flows close to baffle joints.

[11] Crud Induced Localised Corrosion – an accelerated form of corrosion that has historically resulted in a large number of failures in *BWR*s. Three parameters are involved in this corrosion phenomenon, namely: 1) Large Cu coolant concentrations as a result of e.g., aluminium brass condenser tubes, 2) Low initial fuel rod surface heat flux – occurs in Gd rods and 3) Fuel cladding that shows large initial corrosion rates- occurs in cladding with low resistance towards nodular corrosion.

[12] This corrosion phenomenon resulted recently in a few failed rods. The mechanism is not clear but seems to be related to galvanic corrosion. This corrosion type may occur on the fuel cladding in contact or adjacent to a dissimilar material such as Inconel. Thus, this accelerated type of corrosion occurred on the fuel cladding material at spacer locations (the spacer springs in alloy *BWR* fuel vendors fuel are made of Inconel). Water chemistry seems also to play a role if the fuel cladding material microstructure is such that the corrosion performance is poor. Specifically coolant chemistry with low Fe/(Ni-Zn) ratio seems to be aggressive (provided that the cladding material shows poor corrosion performance. A fuel cladding material with good corrosion resistance does not result in *ESSC*, enhanced spacer shadow corrosion, even in aggressive water chemistry.

The failure statistics up to 2001-2004 were presented in the IZNA-4 Annual Report, Figure 9-1 to Figure 9-2. The failure statistics for the year 2004 in these figures are preliminary.

Most of the US BWR failure cases are related to crud-accelerated corrosion failures. Other US BWR failure cases involved six plants, which experienced PCI-like failures following control rod moves. Debris fretting also remains a problem even after the introduction of debris filters.

In PWRs the primary contributor to failure rates remains grid-to-rod fretting; however, experience with new grid designs appears to be promising. Last year it was noteworthy that some PCI-suspect failures were also experienced at three B&W-designed PWR plants following the movement of axial power shaping rods (APSRs) even though their calculated stress levels remained within the permissible range.

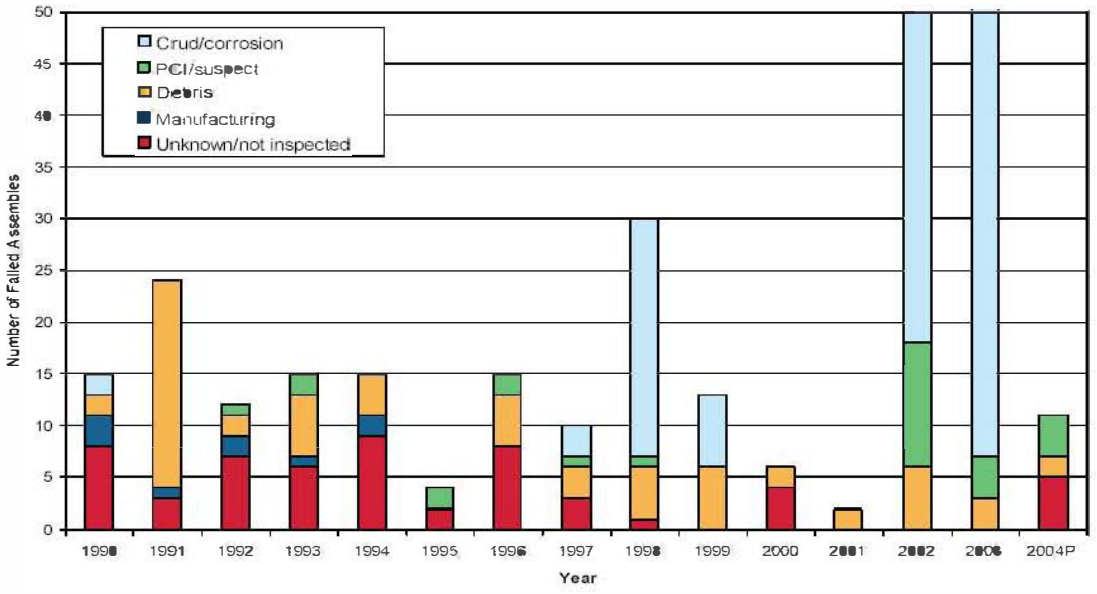

Figure 9-1: Trend in US failure root causes (2004 results are incomplete), Yang et al., 2004.

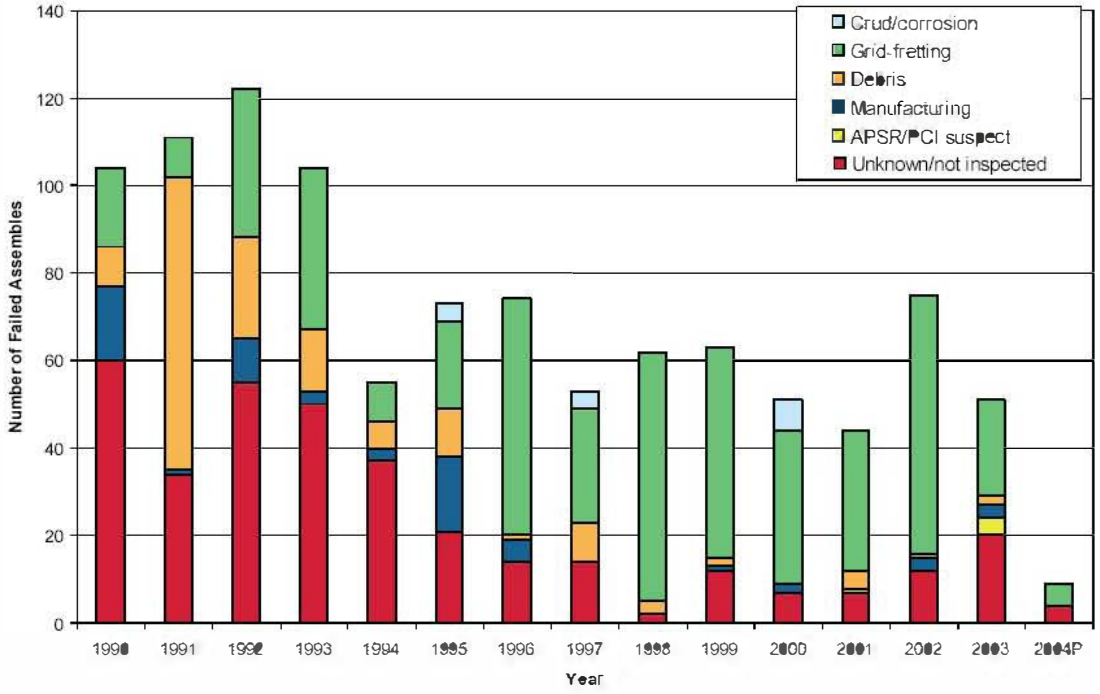

Figure 9-2: Trend in US *PWR* failure root causes (2004 results are incomplete), Yang et al., 2004.

In the European BWRs debris fretting is one of the major failure causes. Debris filters in the BWR fuels do not eliminate the debris fretting failures while the debris filters seems to be efficient in the PWRs.

Table 9-2 and Table 9-3 provide key data for some of the most recent fuel-failure cases.

10 CLADDING PERFORMANCE UNDER ACCIDENT CONDITIONS (PETER RUDLING)

10.1 INTRODUCTION

Three different design basis accidents are treated in this section: (i) Loss Of Coolant Accident, *LOCA*, (ii) Anticipated Transient Without Scram, ATWS, and, (iii) Reactivity Initiated Accident, *RIA*.

10.1.1 LOCA

Several parameters are impacting the fuel performance during a *LOCA*, outlined in Figure 10-1.

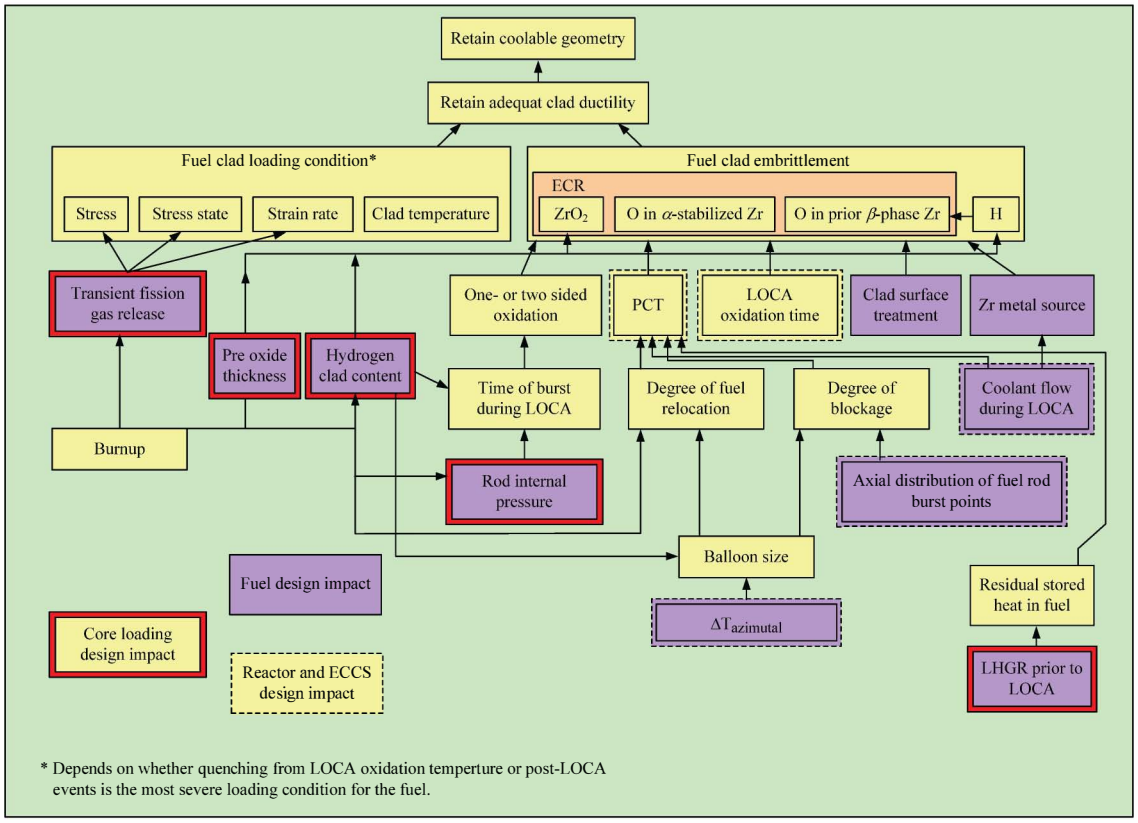

Figure 10-1: Parameters Impacting *LOCA* fuel performance.

The interested reader is referred to the *ZIRAT*-9/*IZNA*-4 Special Topics Report on *LOCA and RIA in BWRs and PWRs,* Rudling et al., 2004/2005 for more details.

10.1.1.1 Reactor kinetics

Loss-of-coolant accidents can be differentiated between several categories depending on the size of the postulated break in the primary coolant system.

For the design basis accident a Large Break Loss of Coolant Accident, *LBLOCA*, - a "guillotine" (or double-ended) break is postulated on one of the cold legs of a *PWR*, or in one of the recirculation pump intake lines of a *BWR*. A small break *LOCA* covers the spectrum of events where the break in the primary circuit is less than a major one and does not necessarily lead to rapid blow-down and complete uncovering of the core.

During a *LBLOCA*, the primary system pressure drops and all the reactor water is expelled into the containment. The drop in pressure would activate the protection system and the reactor would be tripped. The fission chain reaction in the core would thus be terminated, however, decay heat would continue to be released at a high rate from the fuel. The various Emergency Core Cooling Systems, *ECCS* subsystems must then provide sufficient cooling to minimize overheating and fuel cladding damage.

10.1.1.2 Fuel behaviour during LOCA

The fuel rod behaviour during the *LOCA* event is schematically shown in Figure 10-2

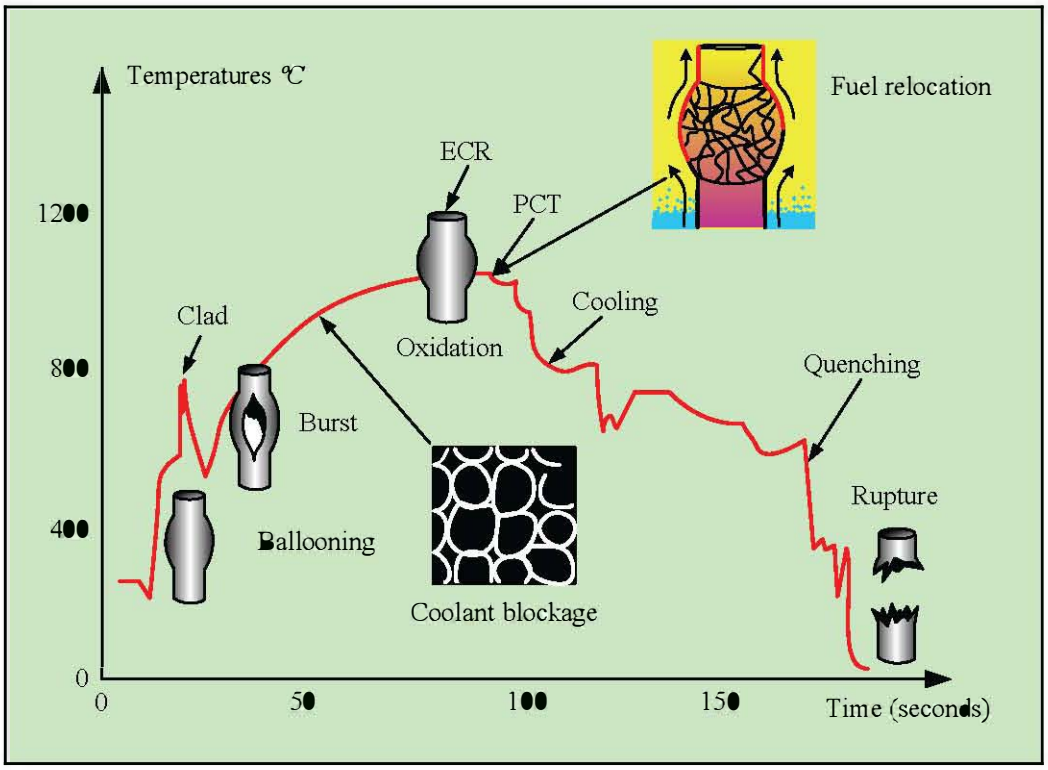

Figure 10-2: Typical *LBLOCA* in a *PWR*.

and can be separated into three different phases:

- **Ballooning** - The loss of coolant results in a dramatic increase in fuel clad temperature. Large plastic strains, ballooning, of the fuel claddings may occur due to the high clad temperature and large clad stresses[19].

  Ballooning of the fuel rods may result in blockage of the coolant sub-channel that in turn may impact the fuel coolability. If large fuel clad burst strains occur at the same axial elevation, *co-planar deformation,* in the fuel assembly, the coolability may be significantly degraded. Specifically, the clad azimuthal temperature gradient will strongly impact the burst strain. After a certain amount of plastic deformation the fuel rod may burst allowing steam to get inside the fuel rod. The fuel clad axial temperature distribution will determine the burst axial elevation of the fuel rods in the assembly. This axial and azimuthal fuel clad temperature distribution is in turn dependent on heat transfer mechanisms at the surfaces of the cladding.

  The majority of current data on fuel clad ballooning and effects on coolant *blockage*[20] were obtained in single- and multi-rod out-of-pile and in-pile tests of low burnup rods by different types of heating. In these tests, clad burst strains up 90% were seen. *It is interesting to note that no LOCA experiment with a multi-rod array and simulated reflood cooling has yet produced fuel clad deformations which would inhibit fuel rod cooling*. Comparing the results obtained in different tests (single-rod versus multi-rod tests and unirradiated fuel in out-of-pile versus irradiated fuel in in-pile tests) it appears that the fuel clad ballooning behaviour and the two-phase thermal-hydraulic impact on blockage is complex and difficult to foresee and model.

  Another point that has not been completely resolved is how the significant microstructural changes (e.g. fuel clad bonding, formation of pellet rim zone, transient fission gas release, etc.) occurring in fuel pellets with burnups exceeding 50 MWd/kgU will impact fuel rod LOCA performance.

  Ballooning may also result in fuel relocation[21] *that may impact the cladding temperature as well as the Equivalent Cladding Reacted, ECR in the later phase of LOCA. The exact impact of fuel relocation in high burnup fuel on peak cladding temperature and ECR needs however to be assessed.*

---

[19] The large clad stresses results from the large fuel rod internal overpressure due to the loss of the system pressure
[20] Blockage (%) = 100X [(Difference in cross-section between ballooned and non-ballooned rod)/(original coolant channel cross-sectional area)].
[21] Fuel relocation may occur, if during *LOCA* a section of the fuel rod experiences ballooning, by slumping of fuel fragments from upper location in the ballooned section.

11 FUEL RELATED ISSUES DURING INTERMEDIATE STORAGE AND TRANSPORTATION (ALFRED STRASSER)

11.1 INTRODUCTION

The permanent disposal of spent nuclear fuel has yet to become a licensed reality in countries that generate nuclear power, although most countries are in the process of developing criteria, designs and identifying sites with this objective. Meanwhile the spent fuel pools at the nuclear plant sites are filling up with spent fuel and the utilities are transferring the spent fuel from the pools to dry cask storage sites that are located, mostly, at the plant sites as well.

Exceptions are the central, large intermediate pool facilities that serve all the plants in Sweden (CLAB facility) described in previous *ZIRAT* reports and all the plants in Finland at the Olkiluoto plants (TVO-KPA-STORE) and at the Loviisa plants (Loviisa-KPA-STORE), Kukkola, 2001. An interesting economic analysis made by Kukkola at that time, comparing the costs of pool expansions vs. dry cask storage, concluded that expansion of the pool storage was more economical. The relative cost differences are shown in Table 11-1, with the value 1.00 assigned to pool storage without densified racks. *These analyses favoring dry storage must be site specific since analyses (Japanese) given in past ZIRAT reports give the reverse ratings while KKGösgen's evaluation of some time ago also favored pool storage.*

Table 11-1: Comparison of Relative Pool vs. Dry Cask Storage Costs, Kukkola, 2001.

Extension alternative	30 years plant operating time	45 years plant operating time
Water pool storage extension with open fuel racks	1,00	1,00
Water pool stoarge extension with dense fuel racks	1,42	1,32
Cask storage at ground level	5,45	5,35
Cask storage in VLJ repository	5,79	5,59
Dry vault storage MVDS	4,76	3,95
Dry vault storage FUELSTOR	5,00	2,68
Dry vault storage NUHOMS	3,18	2,97
Dry vault storage MACSTOR	2,00	1,76
Water pool storage in VLJ repository	5,50	3,19

The US nuclear plants will run out of pool storage space in about 2013 and as a result all the plants have or are planning to have dry storage facilities, or independent spent fuel storage installations (ISFSIs). As of the beginning of 2006 there were 33 ISFIs to service 55 plants with 18 ISFIs planned to service 27 plants, Supko, 2006. The location of the US ISFIs, the number of casks at each site and the type of license they hold are shown on Figure 11-1.

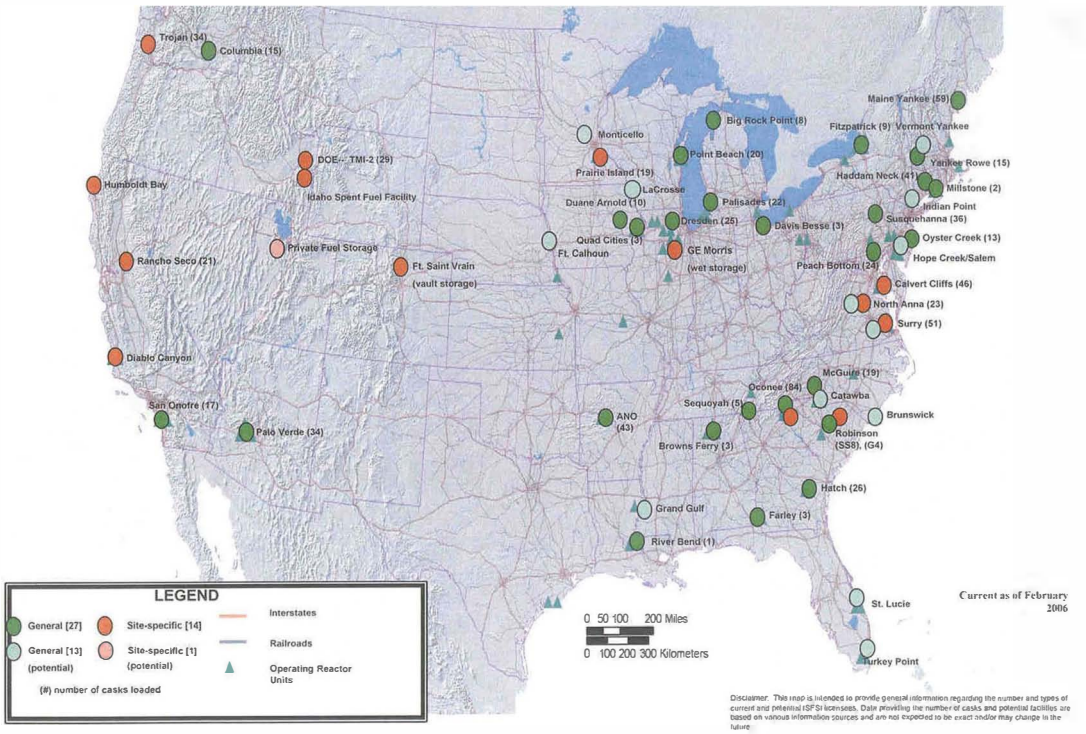

Figure 11-1: Current and Potential Independent Spent Fuel Storage Installations, Brach, 2006.

The total amount of spent fuel in the US is about 54,000 tons of heavy metal, of which 8,500 tons are stored in 800 dry storage casks. At the rate of 2,000 tons of spent fuel discharged per year, a total of 24,000 tons would have to be in dry storage by about 2015 representing about 1/3 of all spent fuel in dry storage. The fuel discharge rate would fill 200 storage casks per year. The projection for dry storage levels to the year 2020, assuming no additional nuclear plants and no available permanent disposal sites, are shown in Figure 11-2.

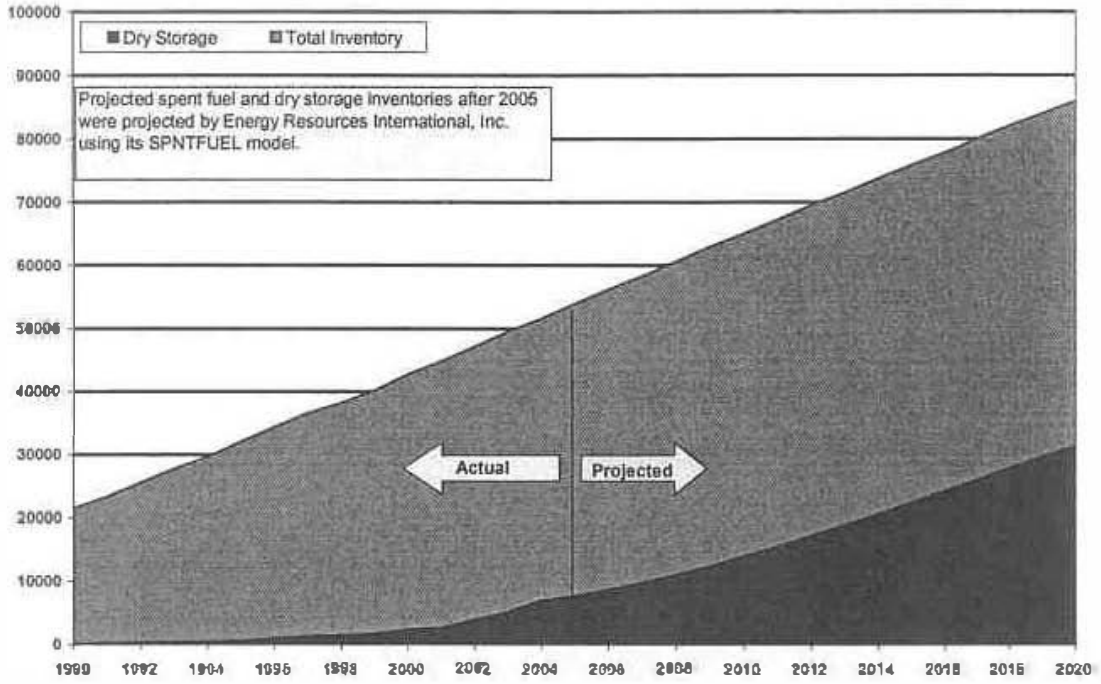

Figure 11-2: Cumulative US Commercial Spent Nuclear Fuel Inventory (1990 to 2020) Spent Nuclear Fuel (Metric Tons Uranium), Supko, 2006.

The intermediate storage has clearly become a significant business and a seemingly permanent part of the fuel cycle. Even the opening of Yucca Mountain, "officially" scheduled for 2018 at this time, would require the maintenance of these intermediate storage sites for the foreseeable future unless a central, intermediate storage site becomes in existence.

The nuclear plants outside the US will discharge about 9,000 t/yr, of which about a quarter will probably be reprocessed, leaving about 7,000 t/yr to be placed into storage. As an example, the intermediate storage summary for Germany is shown on Table 11-2.

12 POTENTIAL BURNUP LIMITATIONS

12.1 INTRODUCTION

The potential fuel assembly burnup limitations related to zirconium alloy components are summarized in this Section. The burnup limitation that have actually been reached, but have been or are being extended, are:

- Corrosion limits of Zry-4 in high power *PWR*s, are extended by the alternate use of improved cladding alloys. Improved corrosion performance by the new alloys may allow the utilities to use the added margins, to modify plant operation e.g., to lower fuel cycle cost. However, this modified operation will in most cases result in higher corrosion duty of the zirconium materials. Thus, it is believed that the corrosion may always be limiting for plant operation even with the new type of alloys. Furthermore, the influence of *CRUD* on corrosion may increase with increasing duty.

- Bowing of *PWR* fuel assemblies contributed in part by irradiation growth, creep and hydriding of Zry-4, has been reduced by improved guide tube materials (i.e., lower irradiation growth and hydriding rates), reduced assembly holddown forces, and other mechanical/themomechanical design changes, but not yet finally eliminated.

- Bowing of *BWR* channels, extended by improved manufacturing processes, design changes such as variable wall channel thickness with relatively thicker corners, and in-core channel management programs.

- *RIA* and *LOCA* related burnup licensing limits are in the process of being assessed by additional experimental data and analyses. It would appear that the current *LOCA* limits are sufficiently conservative for fuel burnups up to 75 MWd/kgU. The *RIA* limits (threshold enthalpies) may continue to decrease as a function of burnup due to the increase in clad corrosion and hydrogen uptake.

- The categories of event likely to eventually limit reliably and safely achievable burnup levels are outlined below. The zirconium alloy component most sensitive to the limits and potential methods for extending the limits are noted below.

12.2 CORROSION AND MECHANCIAL PROPERTIES RELATED TO OXIDE THICKNESS AND H PICKUP

- *BWR*s: increased uniform and shadow corrosion, oxide thickness spalling, increased hydrogen pickup, and formation of radial hydrides due to longer residence time, higher power, modern power histories, and water chemistry changes. Current crucial issues are: shadow corrosion mechanisms its effect on channel bow, late increased corrosion and hydrogen pickup of Zry-2 at high burnups, and formation of radial hydrides, *CRUD*-chemistry-corrosion interaction, effect of water chemistry impurities, as well as specific effects of *NMCA* with or without Zn-injection.

- *PWR*s: increased uniform corrosion, oxide thickness, spalling, and new Zr alloys due to longer residence time and higher Li, higher power, more boiling. The development of new Zr-alloys is still ongoing. The data base for several of the new alloys is still limited. Zr-Nb alloys are occasionally affected by accelerated corrosion due to surface contaminations and/or boiling. Welding of the new alloys may need improved processes (Zr-Nb alloys) and chemical compositions between dissimilar metals such as e.g. *ZIRLO* and Zry-4 may result in inferior corrosion resistance. Luckily, the corrosion temperatures at these elevations in the core are significantly lower than the peak temperatures.

- Decreased ductility and fracture toughness as consequence of the increased hydrogen pickup during any situation (e.g., *RIA*, *PCMI*, *LOCA* and post-*LOCA* events, seismic event, transport container drop-accident conditions),

- Increased growth due to higher hydride volume and thick oxide layers.

- Increased corrosion due to impact of hydrides at the cladding outer surface.

- Impact of corrosion and hydrogen pickup on creep behaviour of fuel claddings during class 1-IV events and during intermediate storage.

- Increased effects of irradiation and hydrides on the fracture toughness of thin-walled zirconium alloy components.

Most sensitive component

Spacer and fuel claddings.

Increase margin for *PWR*

- Improved knowledge of corrosion and hydrogen pickup mechanisms.

- Improved alloys with appropriate fabrication processes: *ZIRLO*, *MDA*, *NDA*, and M5/Zr1Nb. Duplex is another alternative that may be necessary to achieve satisfactory mechanical properties.

- Zr-alloys such as Optimised *ZIRLO*, Modified *MDA*, S2, Modified E635 with reduced Sn content in comparison to the original composition of *ZIRLO*, *MDA*, *NDA* and E635 are being explored.

- Change to enriched B soluble shim to reduce Li. There is however a fear that enriched B would increase *AOA* potential, i.e., more absorption per g. B, even though there may be less B.

- Improved water chemistry and *CRUD* control.

- Increase corrosion resistance of steam generator materials.

Increase margin for *BWR*

- Improved knowledge of corrosion and hydrogen pickup mechanisms at high burnups.
- Modification of manufacturing processes (to get optimum sized, more stable second phase particles).
- Zry-4 fuel channels for controlled positions
- Improved alloys under development.

Improved water chemistry and *CRUD* control.

12.3 DIMENSIONAL STABILITY

- Increased dimensional changes of components and differential dimensional changes between them resulting in reduced fuel rod spacing or even rod contact, guide tube bowing, fuel assembly bowing, spacer cell and envelope dimensions, *BWR* fuel channel and *PWR* fuel assembly bow may result in:
  - decreased thermal margins (*LOCA* and dry-out)
  - control rod insertion difficulties (safety issue)

Most sensitive component

Potentially all zirconium alloy components, but currently *PWR* guide tubes and *BWR* channels. Also *BWR* spacers have occasionally increased so much in dimensions that unloading of the assembly from the outer channel was very difficult.

Increase margin for *PWR*

- Alloys with lower growth and hydriding rates for guide tubes – *ZIRLO*, M5, E635 (Anikuloy).
- Modified mechanical design to provide lower hold-down forces, stiffer assemblies, etc.
- Beta-quenched material after the last plastic deformation step during manufacturing. (Beta-quenched materials do normally, however, show higher corrosion rate and lower ductility. These properties might be improved by an appropriate final heat-treatment in the alpha-phase. Also applies o *BWR* materials).

Increase margin for *BWR*

- Uniform microstructure and texture throughout the flow channel.
- Use of lower growth material, such as beta-quenched material in as-fabricated step, NSF or other Nb-modified zirconium alloys.
- Channel management programs, including assessment of degree of control over specific reactor periods.